Tampere University

Ali Tayyib Göktas

JOINT COMMUNICATIONS AND SENSING DESIGN FOR BEYOND 5G SYSTEM

Master of Science Thesis
Faculty of Information Technology and Communication Sciences
Examiners: Assistant Prof. Bo Tan
December 2022

ABSTRACT

Ali Tayyib Göktas: Joint Communications and Sensing Design for Beyond 5G System
Master of Science Thesis
Tampere University
Master's Degree Programme in Computing Sciences
December 2022

Joint communication and sensing (JCAS) is an emerging research topic aiming to integrate radio communications and radar systems in time and frequency domains along with the spatial domain. Integration in the spatial domain relies on a suitable beamforming technique for acquiring desired detection performance levels for both operations. Beamforming methods in the context of JCAS systems, with an emphasis on convex optimization, are studied in this thesis. A previously established work on beamformer design for optimum antenna selection is reviewed and duplicated to establish the groundwork for the main research. The novel beamforming algorithm proposed in this work maximizes the detection performance for the radar function in a JCAS system while maintaining the communication performance at an acceptable level. This is accomplished in the presence of clutter and with no assumption of a direct path between the transmitter and the communication user. A mathematical groundwork is presented for acquiring a valid convex optimization problem to represent the beamforming objective and constraints, along with using rank one decomposition to convert the result into a beamforming weight vector usable in practical application. The tests performed on a simulation environment showed that performance tradeoffs between radar and communication functions are observable on acquired results, in addition to assurance about the validity of assumptions made during problem definition.

Keywords: JCAS, JRC, beamforming, convexity, optimization

PREFACE

This thesis is a part of research work on joint sensing and communication schemes for the future radio systems, which is conducted by the electrical engineering unit of Tampere University, and led by Prof. Mikko Valkama. The work on the content presented in this thesis has started in March 2022, supervised by Asst. Prof. Bo Tan, and was set on course by an idea regarding the acquisition of a globally optimum solution for a beamforming problem that was only solved with a local optimum before, proposed by Dr. Mateen Ashraf. I am grateful to Bo for his professional guidance and friendly attitude during the whole process and to Mateen for teaching and advising me about both technical topics, and how to conduct research in general.

I would also like to thank my beloved family for their love and support during my whole life. In addition, I thank all of my friends in Tampere for coloring my life with their company, along with my old friends in Turkey who kept correspondence with me.

Tampere, 20th December 2022

Ali Tayyib Göktas

CONTENTS

LIST OF SYMBOLS AND ABBREVIATIONS

ADC	Analog to Digital Converter
DFRC	Dual Function Radar Communications
DR	Detection Rate
FAR	False Alarm Rate
FIR	Finite Impulse Response
IoT	Internet of Things
JCAS	Joint communication and radio sensing
JCR	Joint Communications and Radar
JRC	Joint Radar and Communications
LNA	Low Noise Amplifier
MAC	Medium Access Control
mmWave	Millimeter Wave
MVDR	Minimum Variance Distortionless Response
PDF	Probability Distribution Function
PMN	Perceptual Mobile Network
QAM	Quadrature Amplitude Modulation
RadCom	Radar-communications
RF	Radio Frequency
SCNR	Signal to Clutter and Noise Ratio
SDR	Software Defined Radar
SNR	Signal to Noise Ratio

1. INTRODUCTION

The past decade has seen rapid development of research on coexistence, co-operation, and co-design of radio communication and radar systems. These technologies have been developing in parallel for decades before starting to intersect more and more in contemporary research. Instances of commonalities between radar sensing and radio communication include partially overlapping system architecture[1], circuitry[2], and signal processing techniques[3]. These correspondent features have been among the motivating factors behind the research on joint radar and communication systems, alongside the concern on efficient bandwidth usage, which was also among driving forces behind research on co-existence, i.e. a lower level of integration, between communication and radar systems[4]. Co-existence of radar and radio communication systems relies on each system treating the signal from the other as interference and attempting to mitigate them. A higher level of integration is achievable with co-operating radar and communication systems that share information with each other for performance improvements. One popular approach to achieve this goal is to utilize passive sensing for the radar functionality[5], which relies on the radar system receiving signals from other radio transmitters, for example, Digital Video Broadcasting (DVB), 802.11 access point (AP). This approach has several issues, including the strong direct path signal leakage on the surveillance channel, in addition to the problem that the only way to know signal waveform is to tap off from the reference channel.

The problems mentioned above could be overcome by increasing the integration level of radar and radio communication systems, by co-designing them rather than aiming for mere co-existence. Joint communication and sensing (JCAS) is a co-design solution that utilizes a jointly designed common transmit signal for both purposes and possibly shares most of the receiver hardware except signal processing algorithms[2]. JCAS differs from other spectrum-sharing concepts by using a fully shared transmitter in addition to a largely shared receiver that consists of components such as frequency mixers, phase shifters, and low-noise amplifiers. This allows JCAS systems to have higher spectral efficiency than systems designed with other spectrum-sharing concepts while also causing the waveform design aspect of the system to be more complicated. Design and optimization of the transmit waveform are among the main challenges of designing a JCAS system since the transmitted signal is required to carry information efficiently to communication receivers and illuminate radar targets with high enough power radiation for maximizing detection performance while keeping the receiver processing from being too complex.

There have been numerous works on co-designed radar and communication systems under different names, including JCAS, Radar-communications (RadCom), joint radar and communications(JRC), joint communications and radar(JCR), and dual function radar communications(DFRC). The terms JRC and JCR are occasionally used to imply the priority of radar operation over the communication operation or vice versa, respectively, in co-designed systems. Throughout this thesis, the term JCAS will be used for joint radar and communication systems in general, and the term JRC will be used when referring to JCAS systems that prioritize the radar operation over communication operation, in the sense that main beam is allocated for radar operation, as in the case of Chapters 3 and 4. Research on JCAS systems, in general, aims to increase the level of integration in time and frequency domains, in addition to the spatial domain. This thesis work contributes to spatial domain integration and, more specifically, beamforming for JCAS systems.

A good beamforming algorithm is an integral part of designing the optimal JCAS waveform since weights of antenna array elements can be optimized for providing the best possible signal-to-clutter and noise ratio (SCNR) for the radar target detection while keeping an acceptable signal-to-noise ratio (SNR) for the communication operation in JCAS systems. Beamforming studies within the context of JCAS systems aim to increase the integration of radar and communication components in the spatial domain, complementing the studies on time and frequency domain integration. This thesis work focuses on beamforming in the context of JRC systems and approaches two different problems with objectives of minimizing the usage of RF chains, and maximizing the detection performance, respectively, while providing a novel method for solving the latter problem under specific conditions.

Beamforming is the problem of assigning suitable weights for each element in an antenna array system to achieve desired gain levels for signals radiated to or received from different spatial locations. This concept is analogous to a linear spatial FIR filter since beamformers weights and linearly combine the sensor inputs that correspond to different spatially sampled signals. In this thesis, Convex optimization techniques are used for finding the optimal beamforming weights in Chapter 3 and Chapter 4. Specifically, the critical steps carried out to achieve this goal include:

1. Mathematical formulation of the optimization problem,
2. Converting the formulated optimization problem into a convex optimization problem.

Chapter 3 is devoted to finding the minimum number of active antennas to guarantee acceptable performances of the radar and communication systems, as proposed by[6]. This was achieved by having the objective function as an approximation of l_0 norm of the weight vector and setting the constraints so that the antenna pattern at illuminated directions is formed in a way that gain will be no smaller than a set level for radar or communication operations depending on the direction angle. On the other hand, Chapter 4 is aimed at maximizing the radar SCNR while complying with the power constraints and minimum acceptable value of communication SNR. Problem premises is similar to the work in[7] in the sense of having prior information about clutter and utilizing it to improve SCNR on the receiving signal. Unlike the problem in cited work, however, only one non-negligible clutter element has been assumed in this work to achieve the global optimal solution rather than the local optimal as reached in[7]. The steps of manipulating the mathematical expressions in the optimization problem statement to achieve a convex optimization problem are presented in Chapter 4 before applying approximations and rank reduction algorithms on the result to get a vector of beamforming weights. Simulation results are presented at the end of Chapter 4, which characterize the trade-off between radar SCNR and communication SNR, in addition to confirming the validity of the approximations made during problem definition.

The remaining chapters of this thesis are organized as follows: Chapter 2 provides more detailed background on beamforming and JCAS systems. Chapter 3 elaborates on the antenna selection problem for JCAS systems, reviews the solution presented in [6], and presents the results acquired from duplication of the solution method proposed in the reference paper. Chapter 4 contains a thorough explanation of the premises for a JCAS beamforming problem and the approach proposed in this thesis for solving it, in addition to the evaluation of acquired results. Chapter 5 concludes the thesis with a summary of previous chapters.

2. JCAS SYSTEMS AND BEAMFORMING

This chapter provides details about different types of radar and communication systems with different integration levels, alongside the concept of beamforming, to describe where this thesis work fits in. Historical background and previous research on co-existing, co-operating, and co-designed radar and communication systems are summarized in subsection 2.1. Descriptions of the basics of beamforming, definitions of some of the well-known optimal beamformers, and a short introduction to convex optimization are given in subsection 2.2.

2.1 Background on JCAS

Coexistence, cooperation, and joint design of communication and sensing systems is an emerging research topic, mainly motivated by the scarcity of spectrum resources. Due to the fact that those two systems share many commonalities, both in the sense of hardware and signal processing algorithms, it is viable to build multi-purpose systems with both functionalities. This concept can be traced back to works published as early as 1960s [8] where radar pulses were modulated for communication data transmission, albeit with low data rates. Succeeding those works, studies on cognitive radio systems have been done based on secondary users (usually communications users) shaping their spectrum usage around primary users (usually radar users) [9] [10]. Most recent publications in this field are on application-driven systems that strictly require joint radar and communication functionality for their operation, such as the Internet of Things (IoT)[11] and vehicular radar-communication systems [12][13]. Integration of JCAS in mobile networks results in Perceptive Mobile Networks (PMNs) that increase the versatility of mobile networks by granting them the utility of spatial perception, which makes numerous sensing utilities possible with existing mobile network infrastructure. It has been a research topic in recent years[14]. In order to establish where the contributions of this thesis work stand among research on JCAS research, the following subsections will elaborate on different integration levels in the design of those systems.

2.1.1 Co-existing radar and communication systems

Radar and communication systems consider each other as interferers in the case of co-existence. The only difference in system components between the case of separate radar and communication systems operating independently and the case of co-existence is that both systems have their respective canceler components that attempt to mitigate the interference caused by the other system. The information required for mitigating the interference both systems cause on each other is not shared between them but is estimated. The Block diagram in Figure 2.1 depicts a co-existing system with blocks for mitigating the interference caused to each other by radar and communication components.

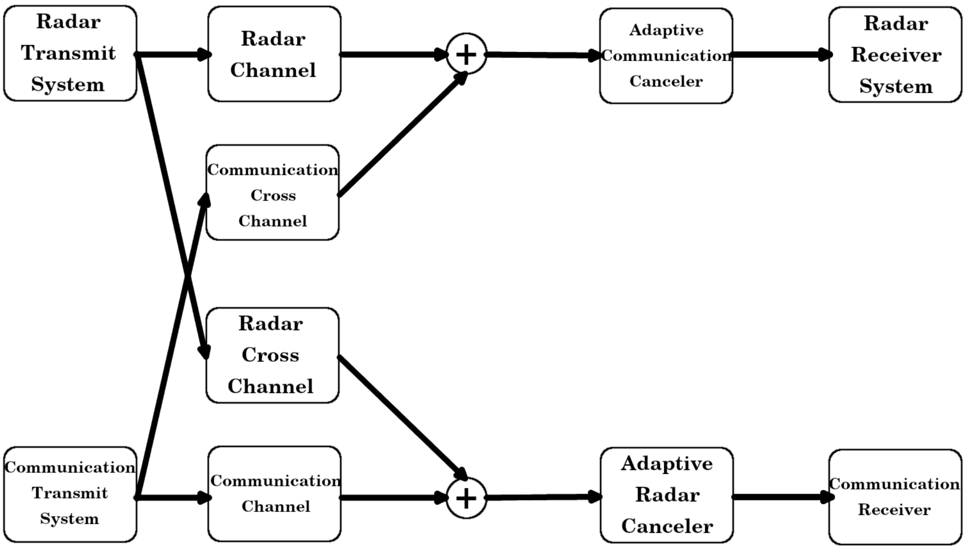

Figure 2.1. *Block diagram representing co-existing radar and communication systems.*

Even though co-existence allows co-located radar and communication systems to operate smoothly within the same frequency band without interfering with each other, the spectral efficiency it provides is limited due to the restrictiveness of interference mitigation methods. A beamforming solution was proposed in [15], where a convex optimization approach was utilized in solving the problem of maximizing radar detection performance while performance requirements for communication operation are met. A cooperative spectrum-sharing approach is implemented in [16], which relies on multi-objective optimization. The interested reader may refer to the survey [4] for a detailed synopsis of research on the co-existence of radar and communication systems.

2.1.2 Co-operating radar and communication systems

Co-operating radar and communication systems treat each other as sources of interference, just as co-existence. Likewise, they operate by employing interference cancellation methods but with the key difference of having shared knowledge from each other. A depiction of this is provided by Figure 2.2. Sharing mechanism may differ by the approach used for cooperation. One prominent example of the type of co-operating radar and communication system is passive radars, which utilize the received information from communication users for the purpose of improving direct path estimation and tracking performances. Another case of sharing mechanism is the usage of radar processing results for the purpose of improving the transmission or receiving equalization for the communication operation.

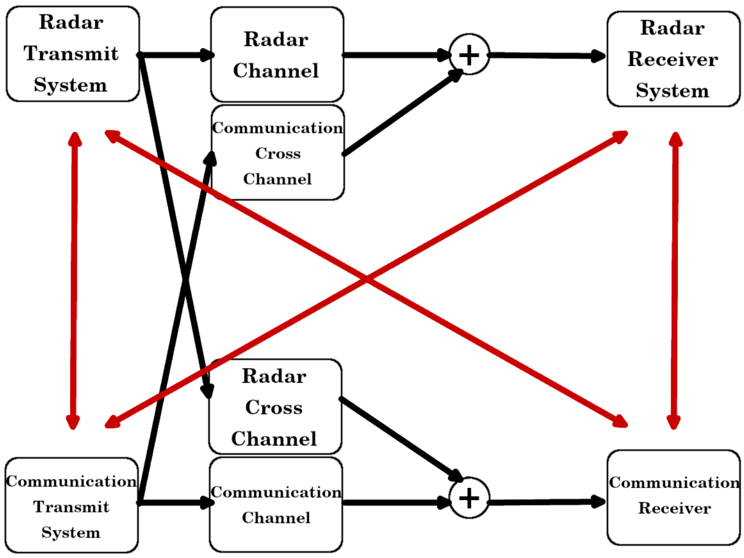

Figure 2.2. *Block diagram representing cooperating radar and communication systems. Red lines indicate information sharing between components.*

Signals of various types may be used for passive sensing. For instance, digital audio broadcast signals are utilized in [17]. Short-ranged detection was performed by passive sensing of WiFi signals in [18]. Microwave links from cellular communication networks have also been used for various passive sensing applications, namely for monitoring weather phenomena such as fog [19] and rainfall [20]. The main ideas behind those works rely on the fact that environmental deviations, including weather changes and the movement of system objects, influence the propagation of radio communication signals. There are, however, two major drawbacks in passive sensing. Coherent sensing is not possible in passive radars since the clock phase of the receiver cannot be known by the transmitter. This leads to difficulties in ranging and joint processing. The other drawback is that the design of the waveform used for communication operation is not known by the passive radar, and differentiating interference and signal is not possible due to that. Taking the performance and spectral efficiency to the next level is possible by using a single waveform designed for both sensing and communication operations, which is coined as the integration level of co-design.

2.1.3 Co-design of radar and communication systems

Co-designed radar and communication systems are jointly developed in all stages. Both systems are considered during design to attain optimal performance for one of the systems while guaranteeing a specified minimum performance for the other system. In this context, high spectral efficiency is achieved with co-designed systems since a single waveform, and therefore the same frequency band is used for both functions. Overall system performance is also further improved by having practically all the information in the system shared between components for radar and communication operations. Communication performance is improved in co-designed systems by channel equalization feedback provided by radar components while sensing performance is enhanced in return by communication users via usage of dedicated codes and modulation for pilot sequences in order to aid the radar operation. A simplified block diagram of such a system is illustrated in Figure 2.3. Co-designed systems generally require elaborate signal processing algorithms and medium access control (MAC) protocols.

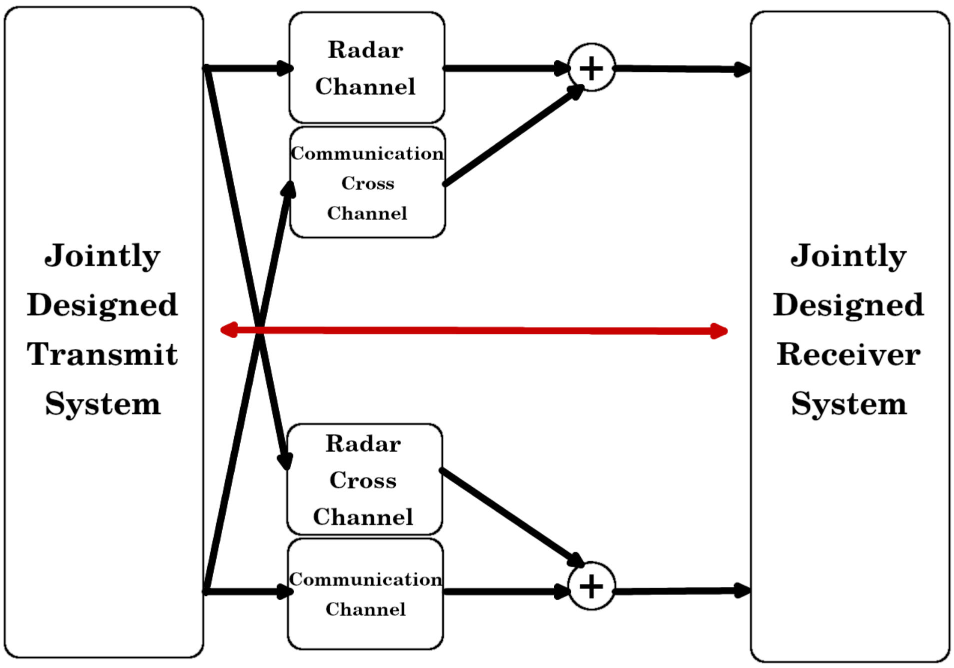

Figure 2.3. *Block diagram representing co-designed radar and communication systems. Red line indicates information sharing between components.*

One of the main factors that separate co-designed systems from lower integration levels and other spectrum-sharing concepts is that co-designed joint radio and communication systems share the majority of the transmitter hardware, in addition to sharing most of the receiver hardware albeit to a lower degree than the transmitter. Exemplary works that could be classified as co-design of radar and communication systems include [21] where a software defined radio (SDR) system was implemented for joint radar-communication operation, [22] where viability of mmWave vehicular communication with infrastructuremounted sensors was studied, and [23] where a PMN system architecture that unifies downlink active sensing, downlink passive sensing, and uplink sensing was proposed.

2.2 Beamforming

The system modality assumed in this thesis for work done in technical chapters is a monostatic broadcast channel[24]. This modality assumes a single transmitter for both radar and communication operations, which transmits a unified waveform for both purposes as depicted in Figure 2.4. One of those operations is carried out in a dependent manner on the other. Either the radar waveform is modulated to carry the information to be communicated across, or the preamble sequence for communication message transmission is used as the radar signal.

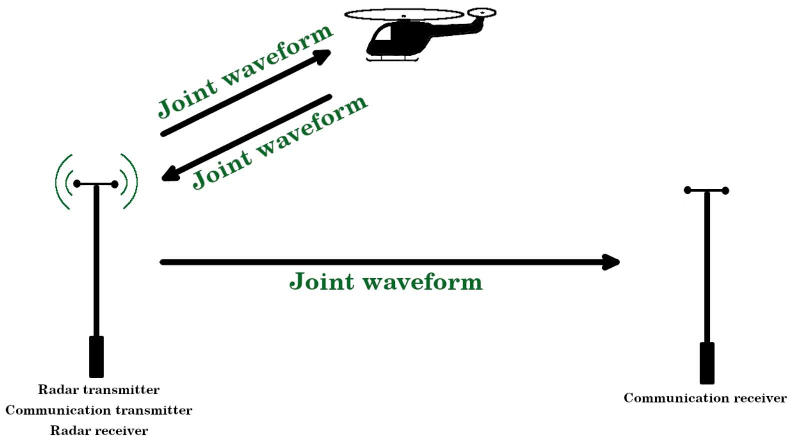

Figure 2.4. *A simple diagram of joint radar and communication operation with the monostatic broadcast.*

While this kind of system has a simplified receiver design, allowing the use of both pulse and continuous waveforms, it can be easily extended to multiple user and target configurations without requiring a complicated MAC protocol. The main drawback of this modality is that it suffers from either the information rate or detection performance being limited[25]. Utilizing highly performing beamforming algorithms is among the ways to compensate for the shortcomings of this modality, and is also an essential part of any joint radar and communication system design that utilizes antenna arrays.

2.2.1 Fundamental beamforming techniques

Beamforming is an array signal processing technique for ensuring an array of antenna elements produces the desired beam pattern, usually to transmit one or multiple spatially directive signals. Particularly in this work, the digital beamforming is investigated, which also refers to precoding. Even though beamforming can be performed both on receive and transmit modes, the rest of this subsection will elaborate on beamformers while assuming they are working on receive mode.

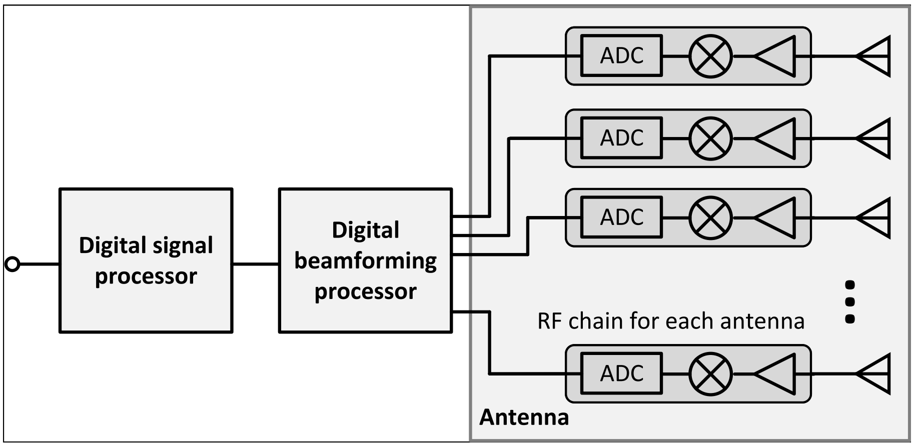

Figure 2.5. *The block diagram used in [26] that shows the fundamental elements of a digital beamformer. The chain of analog-to-digital converter (ADC), frequency mixer, and low noise amplifier (LNA) are commonly referred to as radio frequency (RF) chain.*

A brief schematic digital beamforming system is shown in Figure 2.6. This contrast with analog beamforming, which down-converts and digitizes the summation of all antenna signals using a shared RF chain, each antenna in the digital beamforming system is equipped with an RF chain (LNA, mixer and ADC). In the digital beamforming system, phase shifting and weighting operations are all done in the digital processor. Compared with analog beamforming, full digital operation brings higher flexibility and wideband beamforming by infinite precision digital time delay. It is also viable to approach beamforming as a spatial filtering problem. Similar to how a generic finite impulse response (FIR) filter linearly aggregates the time-sampled signal that the filter is applied, beamformers also produce a scalar output signal by linearly combining the signal that is sampled spatially by each of the receivers[27]. Therefore, just as the main idea of filter design is to acquire the filter coefficients for optimal performance, the principal part of designing a beamforming system is the acquisition of weights allocated for each of the array elements. Optimization methods are a powerful tool in beamforming for that purpose, and specifically, convex optimization is preferred when possible since finding a local optimum is equivalent to finding a global optimum in convex optimization problems.

In an antenna array, if the amplitude and phase weighting for the n^{th} element is shown as

$$w_n = a_n e^{j\theta_n}, \tag{2.1}$$

the output of whole array could be represented as

$$y(k) = \sum_n w_n x_n(k) \tag{2.2}$$

$$= \boldsymbol{w}^H \boldsymbol{x}(k), \tag{2.3}$$

at time k where

$$\boldsymbol{w} = \begin{bmatrix} w_1 & w_2 & \dots & w_N \end{bmatrix}^T \tag{2.4}$$

$$\boldsymbol{x} = \begin{bmatrix} x_1 & x_2 & \dots & x_N \end{bmatrix}^T. \tag{2.5}$$

The optimum beamformers are designed by setting up optimization problems with weight vector $\boldsymbol{w}$ as optimization variables and varying objective functions depending on the type of optimum beamformer. This subsection will include short summaries of three optimal beamformers[27]. For the rest of this subsection, the beamforming weight vector will be denoted by $\boldsymbol{w}$.

- **Multiple sidelobe canceller (MSC)** [28]
  This beamformer consists of a main channel, which is pointed at the desired direction with high gain, and auxiliary channels that are weighted to cancel the interference components in main channel. Its objective function is given by

$$\underset{\boldsymbol{w}}{min}\, E\{|y_m - \boldsymbol{w}^H \boldsymbol{x}_a|^2\}, \tag{2.6}$$

  where $\boldsymbol{x}_a$ is the auxiliary data, y_m is the primary data, and E is the expected value operator. Optimum weights in this beamformer can be shown to be $\boldsymbol{w}^* = \boldsymbol{R}_a^{-1} \boldsymbol{r}_{ma}$ where $\boldsymbol{r}_{ma} = E\{\boldsymbol{x}_a y_m^*\}$ and $\boldsymbol{R}_a = E\{\boldsymbol{x}_a \boldsymbol{x}_a^H\}$. The main drawback of this beamformer is that weight determination depends on the desired signal being received from the main channel only, and not from auxiliary channels.

- **Reference Signal** [29]
  This beamformer relies on having sufficient preliminary knowledge about the desired signal and employing that to create a reference signal used in the objective function of the beamformer optimization problem. The beamforming weights are optimized to minimize the mean square error between the reference signal representing the desired signal and the beamforming output, which is acquired by weighting the array data. The objective function of this beamformer is:

$$\underset{\boldsymbol{w}}{min}\, E\{|y - y_r|^2\}, \tag{2.7}$$

  where y_r is the reference signal, $y = \boldsymbol{w}^H \boldsymbol{x}$ is the array output, and $\boldsymbol{x}$ is the acquired array data. Beamforming weights vector optimized by this method is equivalent to

$\boldsymbol{w}^* = \boldsymbol{R}_x^{-1}\boldsymbol{r}_{xd}$, where $\boldsymbol{r}_{xd} = E\{\boldsymbol{x}y_d^*\}$ and $\boldsymbol{R}_x = E\{\boldsymbol{x}\boldsymbol{x}^H\}$. This beamformer is useful in situations where enough information is known about the desired signal while its direction is unknown.

- **Maximum SNR** [30]
  The objective of this beamformer is to choose weights to maximise signal-to-noise ratio (SNR). This requires preliminary knowledge of desired signal and noise since their covariance matrices are used in the objective function. This beamformer is viable in specific applications. Namely, radar systems are suitable for utilising maximum SNR beamformers since noise can be estimated. At the same time, no detection is performed, and the desired signal is already known since it is transmitted from the radar system itself. The objective function of the maximum SNR beamformer is:

$$\underset{\boldsymbol{w}}{max} \; \frac{\boldsymbol{w}^H\boldsymbol{R}_s\boldsymbol{w}}{\boldsymbol{w}^H\boldsymbol{R}_n\boldsymbol{w}}. \tag{2.8}$$

  If received array data is modeled by $\boldsymbol{x} = \boldsymbol{s} + \boldsymbol{n}$ with $\boldsymbol{s}$ and $\boldsymbol{n}$ being signal and noise components respectively, $\boldsymbol{R_s} = E\{\boldsymbol{s}\boldsymbol{s}^H\}$ and $\boldsymbol{R_n} = E\{\boldsymbol{n}\boldsymbol{n}^H\}$ are the covariance matrices of them. The optimum beamforming weight vector for this beamformer is

$$\boldsymbol{w}^* = \left(\frac{1}{c}\right)\boldsymbol{R}_{nn}^{-1}\boldsymbol{s}, \tag{2.9}$$

  where c is a complex number given by $\frac{\boldsymbol{w}_{opt}^T\boldsymbol{s}}{\boldsymbol{w}_{opt}^T\boldsymbol{R}_{nn}\boldsymbol{w}_{opt}}$. While this beamformer guarantees the true maximization of SNR, its usage is limited because it requires preliminary information on noise and desired signal.

2.2.2 Contemporary research on beamforming for JCAS systems

Numerous works have been published about beamforming methods for joint radar and communication systems. Cramér-Rao bound is employed as a performance metric when setting up the optimization problem for beamforming purposes in [31]. Authors of [32] present beamforming design methods based on a multibeam framework, which they also introduced in the same paper. Another work on multibeam beamforming is presented in [33], where the optimal combination of sub-beams is investigated. The same authors also study the topic further in [34]. Joint radar and communication beamforming in the context of vehicular networks is studied in [35], where roadside units are utilized for the estimation of motion parameters of vehicles as a side benefit of joint radar and communication operation. Likewise, authors of [36] also employ the side benefits of a joint radar and communication system via the use of roadside units and an extended Kalman filtering framework they introduce to increase performance while estimating vehicle states.

Two articles about beamforming problems in joint radar and communication are considered as main references for the next two chapters of this thesis that constitute the main practical work and contribution. The first one is a study on the antenna selection problems in the context of providing the optimal antenna pattern while activating the smallest number of antennas as possible in the antenna array [6]. The authors of this article form an optimization problem that minimizes both transmit power and the number of selected antennas while developing an iterative weighting algorithm to keep the convexity of the problem while including the number of selected antennas as a variable. The work done in this article is reviewed and duplicated in Chapter 3.

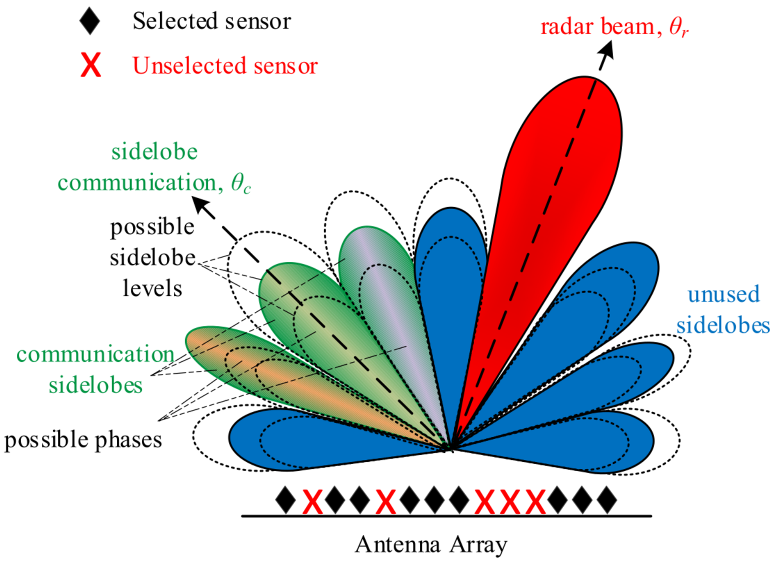

Figure 2.6. *The diagram used in [6] illustrates the antenna selection strategy they propose in the paper.*

The other reference article is [7] in which authors consider a joint radar and communication system model with the indirect path for communication users, which are modelled by channel vectors, and performance is optimized via quadratic programming. Chapter 4 approaches the same problem with a similar model, albeit with the simplification of defining a single clutter source, and proposes a solution method that results in a globally optimal solution, as opposed to [7] in which the modelled problem is solved with a local optimum. The factor that allows the method proposed in this thesis to reach the global optimum is that convexity of the beamforming optimization problem is preserved by a series of mathematical manipulations and substitutions of expressions. At the same time, [7] solves a non-convex problem.

2.2.3 Convexity and convex optimization

Even though many existing optimal beamformers provide well-defined formulas for optimum beamforming weight vectors for different situations, including the ones listed in section 2.2.1, it is not possible to have a formulated solution for every possible system and optimization problem. In most cases, especially when dealing with JCAS systems due to their multi-purpose nature, an optimization problem has to be built from scratch by defining objective functions and constraints regarding the parameters to be optimized and system requirements to be satisfied. In this regard, the main challenge is ensuring that the resulting problem is solvable and provides a globally optimum result. Both of these requirements could be satisfied by utilizing convex optimization, which makes it an invaluable tool in solving beamforming problems. A brief introduction to basic concepts regarding convex optimization is provided in this subsection since convex optimization techniques are employed in Chapters 3 and 4 of this thesis.

A convex function is defined as $f : \mathbb{R}^n \rightarrow \mathbb{R}$ where the domain of f is a convex set, and for all x, y variables from the domain of f, and a θ with $0 \leq \theta \leq 1$, the following inequality holds[37]:

$$f(\theta x + (1-\theta)y) \leq \theta f(x) + (1-\theta)f(y). \tag{2.10}$$

This inequality can be visualised as the line segment between any two points on f lying above the graph of f between those points. Minimization problems with convex objective functions are favourable because finding the local minimum of a convex function is equivalent to finding its global minimum. Solving a maximization problem based on a convex objective function is also possible by changing the sign of the objective function. This is based on the fact that f is concave if $-f$ is convex, and finding the local maximum of a concave function is equivalent to finding its global maximum. This relation between convex and concave functions will be utilized in section 4.2 when approaching the radar SCNR maximization problem.

Mathematically, an optimization problem of minimizing $f_0(x)$ while satisfying the constraints $f_i(x) \leq b_i$, $i = 1, \ldots, m$ and $h_i(x) = 0$, $i = 1, \ldots, p$, which are called inequality constraints and equality constraints respectively, can be written as:

$$min \quad f_0(x) \tag{2.11}$$

$$s.t. \quad f_i(x) \leq b_i,\, i = 1, \ldots, m \tag{2.12}$$

$$h_i(x) = 0,\, i = 1, \ldots, p. \tag{2.13}$$

If the three additional requirements of the objective function f_0 being convex, inequality constraint functions f_i being convex, and equality constraint functions h_i being affine are satisfied for an optimization problem, the problem in question is a convex optimization problem. Stating the beamforming problem objectives as convex optimization problems constitute a central part of the approaches described in Chapters 3 and 4. It should be noted that even if convex optimization cannot directly solve a beamforming problem, it can still make the solution more reachable by providing approximate solutions and a better understanding of the problem. Solution approaches to problems defined in Chapters 3 and 4 utilize iteration and rank reduction, respectively, in tandem with convex optimization.

3. ANTENNA SELECTION

This chapter is focused on the antenna selection problem in the context of JRC systems, and is organized as follows: Section 3.1 describes the model of JRC system. The antenna selection strategy proposed in [6] is summarized in section 3.2, and results acquired from duplication of the proposed strategy are presented in section 3.3. Discussed problems in this chapter and the next chapter are solved with a convex optimization approach.

3.1 System model

The joint system assumed in this problem prioritizes radar operation by assigning the main beam in an antenna pattern and relying on sidelobes for transmission to communication users. Communication messages are transmitted by employing a set of beamforming weights which preserve the optimal antenna pattern but have varying amplitudes and phases, corresponding to different directions of communication users, for each symbol to be transmitted. The approach used here is a quadrature amplitude modulation (QAM) based sidelobe modulation.

The main motivation behind developing an antenna selection algorithm is to reduce the system cost while retaining the performance. The waveform to be transmitted in a JRC system is fed through an array of RF chains, which are expensive, before being passed to the transmit antenna array, which is considerably cheaper component. RF chains contain the circuitry for digital-to-analog conversion, frequency mixing, and power amplification. The antenna selection strategy proposed in the work that is referenced in this chapter assumes a system setup where a smaller number of RF chains are connected to a larger number of transmit antennas and aims to provide a reliable method to decide which antennas should be activated to keep the desired level of performance for both operations while keeping the number of active antennas as small as possible.

The set of angles considered the main lobe direction is denoted as Θ_{rad}. The set of sidelobe direction angles will be denoted as Θ_{sl} during the system model described in this subsection. Any angle belonging to either of those sets is denoted by $\theta_r \in \Theta_{rad}$ and $\theta_\epsilon \in \Theta_{sl}$ respectively. G_r represents the desired gain for radar operation in the main lobe. The phase profile for the main lobe is represented as $\phi(\theta_r)$, a function of

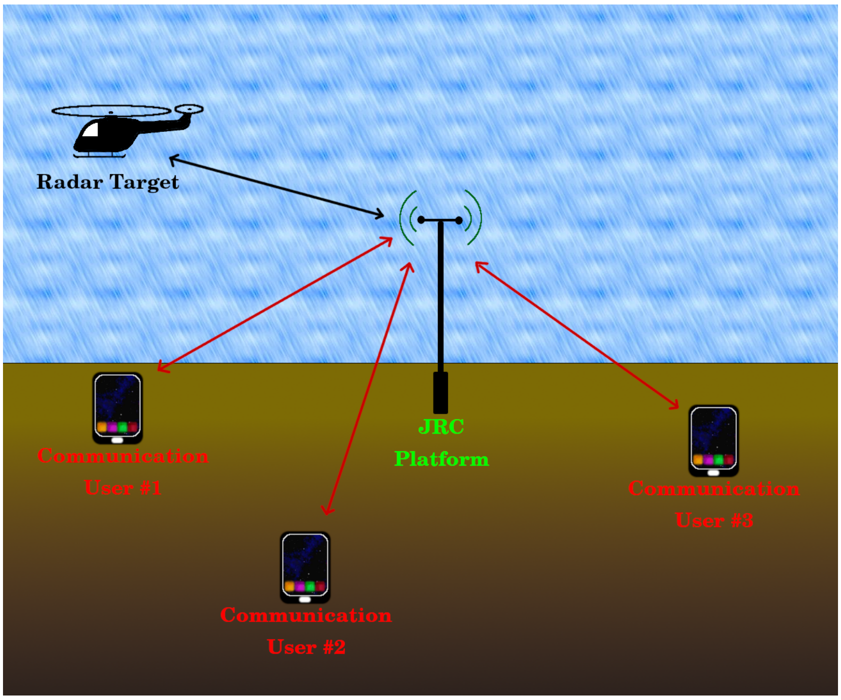

Figure 3.1. *A simple schematic of the JRC system setup.*

θ_r. Let the amplitude and phase to be ensured at direction θ_c for communication symbol coding purposes be denoted as Δ_c and $e^{j\phi_c}$, respectively, where θ_c is the direction of c^{th} communication receiver. The vector of beamforming weights is represented as $\boldsymbol{w}$, and the array response vector for the transmit antenna array when transmit direction is set to θ is shown as $\boldsymbol{a}(\theta)$. With these parameters, an optimization problem for acquiring the $\boldsymbol{w}$ vector for the best possible performance can be stated as:

$$\min_{\boldsymbol{w}} \max_{\theta_r \in \Theta_r} |G_{rad} e^{j\phi(\theta_r)} - \boldsymbol{w}^H \boldsymbol{a}(\theta_r)|, \tag{3.1}$$

$$\text{s. t. } |\boldsymbol{w}^H \boldsymbol{a}(\theta_\epsilon)| \leq \epsilon_{sl}, \quad \theta_\epsilon \in \Theta_{sl}, \tag{3.2}$$

$$\boldsymbol{w}^H \boldsymbol{a}(\theta_c) = \Delta_c e^{j\phi_c}. \tag{3.3}$$

The objective function of this problem statement is interpreted as follows: There are varying amounts of absolute valued differences between the desired values and acquired values of gain and phase at each θ_r direction in the main beam. Objective function (3.1) establishes that the $\boldsymbol{w}$ vector is chosen so that for the θ_r direction with a maximum difference between desired and acquired values, that difference should be as small as possible. Additionally, the constraint (3.2) ensures only a certain amount of maximum gain at sidelobe directions which will be used for communication operation, while constraint (3.3) guarantees the specific amplitude and phase values that correspond to the symbol to be transmitted to the communication user at the relevant direction. The approach to the antenna selection problem referenced in this chapter is based on this optimization problem.

One manipulation that should be done on the problem statement is to convert the min-max problem into a single minimization problem for convexity. This could be done by ensuring via problem constraints that the absolute value difference between the desired beam pattern and the acquired beam pattern is below a certain threshold value for each discrete θ_r value that falls in the main beam direction interval, and modifying the objective function to minimize that threshold. With this modification, problem (3.1)-(3.3) can be equivalently written as:

$$\underset{\boldsymbol{w},t}{min}\; t \tag{3.4}$$

$$\text{s. t. } |G_{rad}e^{j\phi(\theta_r)} - \boldsymbol{w}^H\boldsymbol{a}(\theta_r)| \leq t, \quad \theta_r \in \Theta_r, \tag{3.5}$$

$$|\boldsymbol{w}^H\boldsymbol{a}(\theta_\epsilon)| \leq \epsilon_{sl}, \quad \theta_\epsilon \in \Theta_{sl}, \tag{3.6}$$

$$\boldsymbol{w}^H\boldsymbol{a}(\theta_c) = \Delta_c e^{j\phi_c}. \tag{3.7}$$

This is a convex optimization problem since objective function (3.4) and inequality constraint functions (3.5)-(3.6) are convex functions, in addition to the equality constraint (3.7) being an affine function which necessarily makes it both convex and concave. It is possible to use CVXOPT or another convex optimization solver tool to acquire the optimal $t, \boldsymbol{w}$ values. That value will be a parameter for defining the constraint function about radar performance in the antenna selection problem. The acquired t value will be denoted as γ_{tol} in the upcoming problem definitions.

3.2 Antenna selection strategy

Setting a constant γ_{tol} value as the constraint for the maximum tolerable difference from desired radar antenna pattern frees up the objective function since there is no t variable to be minimized. The antenna selection problem statement takes the form:

$$\underset{\boldsymbol{w}}{min}\; f(\boldsymbol{w}) \tag{3.8}$$

$$\text{s. t. } |G_{rad}e^{j\phi(\theta_r)} - \boldsymbol{w}^H\boldsymbol{a}(\theta_r)| \leq \gamma_{tol}, \quad \theta_r \in \Theta_r, \tag{3.9}$$

$$|\boldsymbol{w}^H\boldsymbol{a}(\theta_\epsilon)| \leq \epsilon_{sl}, \quad \theta_\epsilon \in \Theta_{sl}, \tag{3.10}$$

$$\boldsymbol{w}^H\boldsymbol{a}(\theta_c) = \Delta_c e^{j\phi_c}, \tag{3.11}$$

where $f(\boldsymbol{w})$ will be a convex objective function relating to the number of selected antennas, which depends on the beamforming weight vector. A straightforward approach to building this objective function is to utilize the so-called l_0 norm, which returns the number of nonzero elements of the corresponding vector. There are, however, some issues with directly using an l_0 norm in this problem. Reasons for this will be clarified by comparing

l_0 norm to the definition of l_p norm function, which is defined as:

$$||\boldsymbol{x}||_p := \left(\sum_{i=1}^{n} |x_i|^p \right)^{1/p}, \tag{3.12}$$

where $||\boldsymbol{x}||_p$ is l_p norm, or p-norm, of $\boldsymbol{x}$. All l_p norms are norm functions, and they are convex for $p \geq 1$. These statements follow directly from the defining properties of norm functions in general. Those properties are as follows[38]:

- Norm is nonnegative: $||\boldsymbol{x}|| \geq 0$ for all $x \in \mathbb{R}^n$,
- Norm is definite: $||\boldsymbol{x}|| = 0$ only if $\boldsymbol{x} = \boldsymbol{0}$,
- Norm is homogeneous: $||t\boldsymbol{x}|| = |t|\|\boldsymbol{x}\|$, for all $x \in \mathbb{R}^n$ and $t \in \mathbb{R}$,
- Norm satisfies the triangle inequality: $||\boldsymbol{x} + \boldsymbol{y}|| \leq ||\boldsymbol{x}|| + ||\boldsymbol{y}||$, for all $x, y \in \mathbb{R}^n$.

First, it should be shown that l_p norms satisfy the requirement of norm functions. Nonnegativity, definiteness, and homogeneity properties can be verified trivially by just substituting the l_p norm definition in (3.12) into respective statements. Triangle inequality is more difficult to confirm for the l_p norm case. Still, it has already been proven by Minkowski inequality that L^p spaces are normed vector spaces, which means triangle inequality holds for all l_p norms where $p \geq 1$:

$$\left(\sum_{i=1}^{n} |x_i + y_i|^p \right)^{1/p} \leq \left(\sum_{i=1}^{n} |x_i|^p \right)^{1/p} + \left(\sum_{i=1}^{n} |y_i|^p \right)^{1/p}. \tag{3.13}$$

The fact that l_p norms satisfy the triangle inequality directly implies that they are convex functions. This can be observed by substituting the norm function into (2.10) where the requirement of convexity is defined:

$$||\theta x + (1-\theta)y||_p \leq \theta||x||_p + (1-\theta)||y||_p. \tag{3.14}$$

One can see right away that this inequality holds true based on homogeneity property and satisfaction of triangle inequality by norm functions. However, this still only holds true for $p \geq 1$. Zero norms do not satisfy the homogeneity property for norms and therefore are not norm functions, since they instead satisfy the equality

$$||t\boldsymbol{x}||_0 = \|\boldsymbol{x}\|_0. \tag{3.15}$$

for $t \neq 0$ and this means absolute scalability does not hold for l_0 norms.

Since l_p norms are convex, it is possible to easily define a convex optimization problem that minimizes the transmit power in the form:

$$\underset{\boldsymbol{w}}{min}\; ||\boldsymbol{w}||_2^2 \tag{3.16}$$

$$\text{s. t. } |G_{rad}e^{j\phi(\theta_r)} - \boldsymbol{w}^H\boldsymbol{a}(\theta_r)| \leq \gamma_{tol}, \quad \theta_r \in \Theta_r, \tag{3.17}$$

$$|\boldsymbol{w}^H\boldsymbol{a}(\theta_\epsilon)| \leq \epsilon_{sl}, \quad \theta_\epsilon \in \Theta_{sl}, \tag{3.18}$$

$$\boldsymbol{w}^H\boldsymbol{a}(\theta_c) = \Delta_c e^{j\phi_c}. \tag{3.19}$$

Although the above optimization minimizes the power consumption, it does not ensure the fewest possible number of antennas to be selected. To ensure the optimal antenna selection, one can insert an additional constraint of $||\boldsymbol{w}||_0 \leq M_{max}$ to this problem where M_{max} is the maximum number of allowed antennas. Its optimal value could be found by trial and error. Another option is to modify the objective function into the form $||\boldsymbol{w}||_2^2+\eta||\boldsymbol{w}||_0$ where η is a tuning parameter for setting the balance between the minimum possible transmit power and the minimum possible number of antennas. Since both of these approaches use the non-convex l_0 norm, zero norm statements have to be approximated by convex functions for the problem to be convex. l_1 norm can be utilized for that purpose since it is a convex function and provides the closest approximation of l_0 norm among l_p norms. This leads to the following problem statement:

$$\underset{\boldsymbol{w}}{min}\; ||\boldsymbol{w}||_2^2 + \eta||\boldsymbol{w}||_1 \tag{3.20}$$

$$\text{s. t. } |G_{rad}e^{j\phi(\theta_r)} - \boldsymbol{w}^H\boldsymbol{a}(\theta_r)| \leq \gamma_{tol}, \quad \theta_r \in \Theta_r, \tag{3.21}$$

$$|\boldsymbol{w}^H\boldsymbol{a}(\theta_\epsilon)| \leq \epsilon_{sl} \tag{3.22}$$

$$\boldsymbol{w}^H\boldsymbol{a}(\theta_c) = \Delta_c e^{j\phi_c}. \tag{3.23}$$

The main shortcoming of this approximation is that larger weights in $\boldsymbol{w}$ get penalized more, which would not happen in l_0 norm case. One of the main ideas in [6] is to weight $\boldsymbol{w}$ after the optimization problem is solved based on how much power is allocated at each antenna array element. The problem is solved once more after this weighting, and this time penalization strength is less affected by size of individual weights in $\boldsymbol{w}$. This process is repeated until the number of selected antennas converges or a specified number of maximum iterations is reached. The new problem statement is in the form:

$$\underset{\boldsymbol{w}}{min}\; ||\boldsymbol{w}||_2^2 + \eta\|\boldsymbol{u}^{(i)} \odot \boldsymbol{w}\|_1 \tag{3.24}$$

$$\text{s. t. } |G_{rad}e^{j\phi(\theta_r)} - \boldsymbol{w}^H\boldsymbol{a}(\theta_r)| \leq \gamma_{tol}, \quad \theta_r \in \Theta_r, \tag{3.25}$$

$$|\boldsymbol{w}^H\boldsymbol{a}(\theta_\epsilon)| \leq \epsilon_{sl}, \quad \theta_\epsilon \in \Theta_{sl}, \tag{3.26}$$

$$\boldsymbol{w}^H\boldsymbol{a}(\theta_c) = \Delta_c e^{j\phi_c}, \tag{3.27}$$

where $\boldsymbol{u}^{(i)}$ is the weight vector at i^{th} iteration, and m^{th} element of $\boldsymbol{u}^{(i)}$ is defined as:

$$u_m = \begin{cases} \frac{1}{|w_m^{(i-1)}|}, & \text{if } |w_m^{(i-1)}| > \delta, \\ \frac{1}{\epsilon}, & \text{if } |w_m^{(i-1)}| \leq \delta,. \end{cases} \tag{3.28}$$

where ϵ and δ are very small numbers, and $w_m^{(i-1)}$ is the m^{th} element of $\boldsymbol{w}$ acquired during previous iteration of the problem. δ is used as a comparison point to detect antenna elements that are not selected or, in other words, have practically zero weights. Those antenna elements are ensured to be not selected in the upcoming iteration by setting the weights corresponding to those elements as the large number of $\frac{1}{\epsilon}$. The multiplicative inverse of their magnitude scales the remaining antenna elements selected in the previous iteration to ensure that the optimization problem solver will not be affected by the weight size of individual elements in $\boldsymbol{w}$ when calculating its l_1 norm. This provides a reliable approximation of the l_0 norm while maintaining convexity in the objective function.

Even though utilizing a weighting vector along with l_1 norm is a reliable way to have a convex approximation of l_0 norm, which provides the means for creating an objective function for minimizing the number of selected antennas, the antenna selection is only optimized for the set of constraints given at that time. This is not problematic for constraint functions of θ_r and θ_ϵ as sidelobe, and main beam intervals are expected to be fixed for the whole operating duration. However, transmitted symbol amplitude Δ_c and phase $e^{j\phi_c}$ are expected to change for each symbol to be transmitted to each individual user. For a case with N sets of possible symbols to be transmitted, it will be required to find N beamforming vectors that provide the required performance and have the optimal antenna selection. The weight vector for n^{th} set of transmit symbols and relevant amplitude and phase levels for those will be denoted with the subscript of n for the remainder of this chapter. This leads to the following generalized problem statement for all N cases:

$$\underset{\boldsymbol{w}_n}{min} \; ||\boldsymbol{w}_n||_2^2 + \eta||\boldsymbol{u}^{(i)} \odot \boldsymbol{w}_n||_1 \tag{3.29}$$

$$\text{s. t. } |G_{rad}e^{j\phi(\theta_r)} - \boldsymbol{w}_n^H \boldsymbol{a}(\theta_r)| \leq \gamma_{tol}, \;\; \theta_r \in \Theta_r; \;\; n = 1, \ldots, N, \tag{3.30}$$

$$|\boldsymbol{w}_n^H \boldsymbol{a}(\theta_\epsilon)| \leq \epsilon_{sl}, \;\; \theta_\epsilon \in \Theta_{sl}; \;\; n = 1, \ldots, N, \tag{3.31}$$

$$\boldsymbol{w}_n^H \boldsymbol{a}(\theta_c) = \Delta_{n,c}e^{j\phi_{n,c}}; \;\; n = 1, \ldots, N, \tag{3.32}$$

which means the output for the whole problem should be in the form of a matrix $\boldsymbol{W}$ that has optimal beamforming vector $\boldsymbol{w}_n$ for n^{th} case for its n^{th} column, and with M number of rows where M is the total number of selected and nonselected antenna elements in the system. Using the previously built algorithm N times and acquiring the weight vector for each case separately is a straightforward solution for the generalized problem. However, this is not the optimal approach since selected and nonselected antennas may differ between cases due to the fact that sparsity is enforced separately for each case when the

l_0 norm is approximated for individual weight vectors. This may lead to frequent switching of antennas between on and off states, especially in communication operations with high data rates, which increases the system complexity. In addition to avoiding high system complexity, another advantage of having the same selected and nonselected antenna arrangement between transmit symbols is that the same antennas will be turned off for the whole JRC operation. Those antennas may be utilized for another operation at the same time, which will increase the functionality of RF chains they are connected to.

Another idea in [6] is utilizing the group sparsity concept in building the objective function for the convex optimization problem. Mixed $l_{1,q}$ norm is employed for acquiring a measure of group sparsity in $\boldsymbol{W}$ matrix. $l_{1,q}$ norm is a matrix norm defined as:

$$\|\boldsymbol{w}\|_{1,q} = \sum_{m=1}^{M} \left(\sum_{n=1}^{N} |w_{n,m}|^q \right)^{1/q}, \tag{3.33}$$

where $|w_{n,m}|$ is the weight magnitude of M^{th} antenna element for the transmission of N^{th} communication symbol. Minimization of this mixed norm for $l_{1,2}$ case provides an antenna setup with the same antenna elements with different beamforming weights utilized for each unique symbol transmission. Nevertheless, a weighting function should also be utilized to select antenna elements for each case based on the closest approximation of l_0 norm calculated on the column vector representing that case. Weight function has the same purpose of scaling down the magnitudes of elements in weight vectors while assigning large weights to unselected antenna elements, as in (3.28). This time, the multiplicative inverse of l_2 norm of each row in $\boldsymbol{W}$ is used as a scaling factor for those rows, while the antenna elements assigned very low weights in the previous iteration are scaled up in the same way. The new weight vector, represented as $\boldsymbol{v}$, has its m^{th} element defined by the function:

$$v_m^{(i)} = \begin{cases} \frac{1}{\left(\sum_{n=1}^{N} |w_{n,m}^{(i-1)}|^q\right)^{1/q}}, & \text{if } \sum_{n=1}^{N} |w_{n,m}^{(i-1)}| > \delta, \\ \frac{1}{\epsilon}, & \text{if } \sum_{n=1}^{N} |w_{n,m}^{(i-1)}| \leq \delta. \end{cases} \tag{3.34}$$

Replacing the $l_{1,2}$ norm, along with weighting function, in the previous problem statement results in:

$$\underset{\boldsymbol{w}_n}{min} \; ||\boldsymbol{w}_n||_2^2 + \eta \sum_{m=1}^{M} \left(v_m^{(i)} \sum_{n=1}^{N} |w_{n,m}|^q \right)^{1/q}, \tag{3.35}$$

$$\text{s. t. } |G_{rad} e^{j\phi(\theta_r)} - \boldsymbol{w}_n^H \boldsymbol{a}(\theta_r)| \leq \gamma_{tol}, \;\; \theta_r \in \Theta_r; \;\; n = 1, \ldots, N, \tag{3.36}$$

$$|\boldsymbol{w}_n^H \boldsymbol{a}(\theta_\epsilon)| \leq \epsilon_{sl}, \;\; \theta_\epsilon \in \Theta_{sl}; \;\; n = 1, \ldots, N, \tag{3.37}$$

$$\boldsymbol{w}_n^H \boldsymbol{a}(\theta_c) = \Delta_{n,c} e^{j\phi_{n,c}}; \;\; n = 1, \ldots, N. \tag{3.38}$$

This problem statement minimizes power usage and provides the minimum possible number of selected antennas, in a manner that indices of nonselected antenna elements are consistent throughout each possible set of transmit symbols. The optimization problem has to be solved iteratively until optimal results are obtained while updating the weight function $v_m^{(i)}$ at each iteration. At the initialization stage, all the weights are set to one.

Since the final convex optimization problem is now obtained, the step-by-step process of the antenna selection strategy proposed in [6], and reviewed in this chapter, can be described as follows:

1. Initially, set the weight vector $\boldsymbol{v}^{(0)}$ as a $1 \times M$ vector of ones.
2. Solve the optimization problem defined in (3.35)-(3.38).
3. Update the each element $v_m^{(i)}$ of the weight vector $\boldsymbol{v}^{(i)}$ based on the values acquired from step 2, in accordance to (3.34).
4. If the results converge or the maximum number of iterations is reached, terminate. Otherwise, return to step 2.

3.3 Simulation results

A simulation setup was built based on Algorithm 1 proposed in the reference paper, and acquired results were comparable to the ones presented in reference work. Likewise the reference paper, CVX [39] [40] was the solver tool used for performing these simulations. The main beam allocated for radar operation was set to be directed towards angle $0°$, while the sidelobe region was set as $\Theta_{sl} = [-60°, -7°) \cup (7°, 60°]$. Two communication users were placed in directions $30°$ and $40°$. The simulated antenna array had 40 transmitters, and the maximum allowed sidelobe gain was set to be 20 dB below the main beam gain. After solving the optimization problem described in (3.24)-(3.27) for the simulation setting, the weight vector was updated following (3.28). This was repeated for 5 times in total whereupon convergence occurred. Figure 3.2 shows the number of selected antennas after each iteration. A visualisation of the antenna array profile is presented in Figure 3.3, and transmit beam pattern after convergence is shown in Figure 3.4.

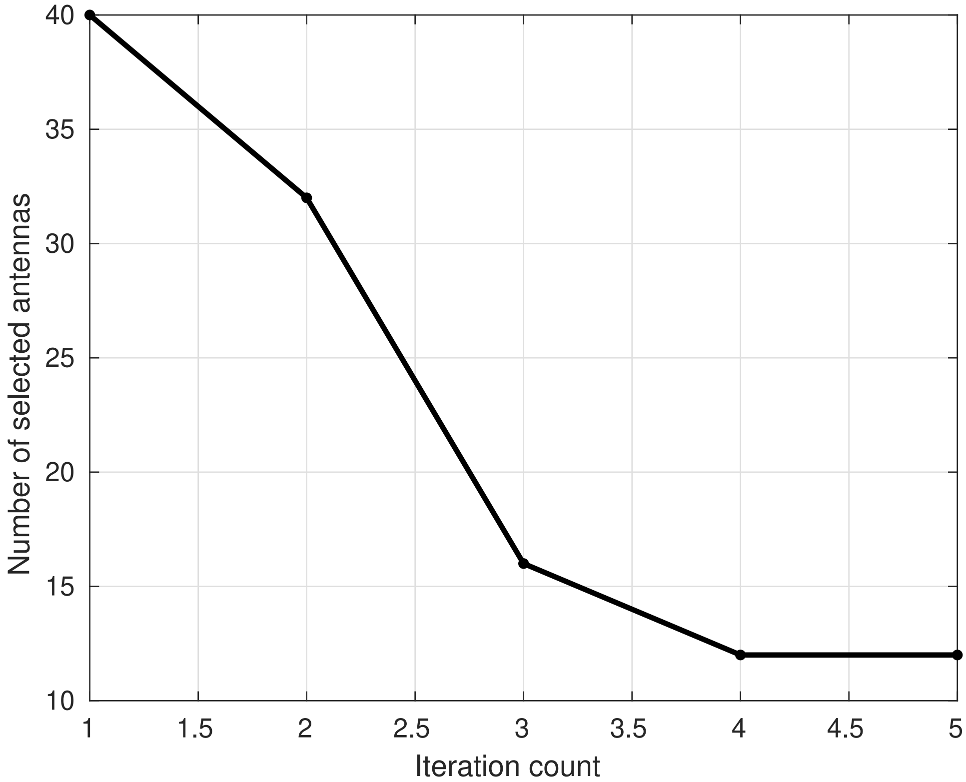

Figure 3.2. *Figure depicting the total number of selected antennas with respect to iteration number. It can be observed that convergence is reached within the first few iterations.*

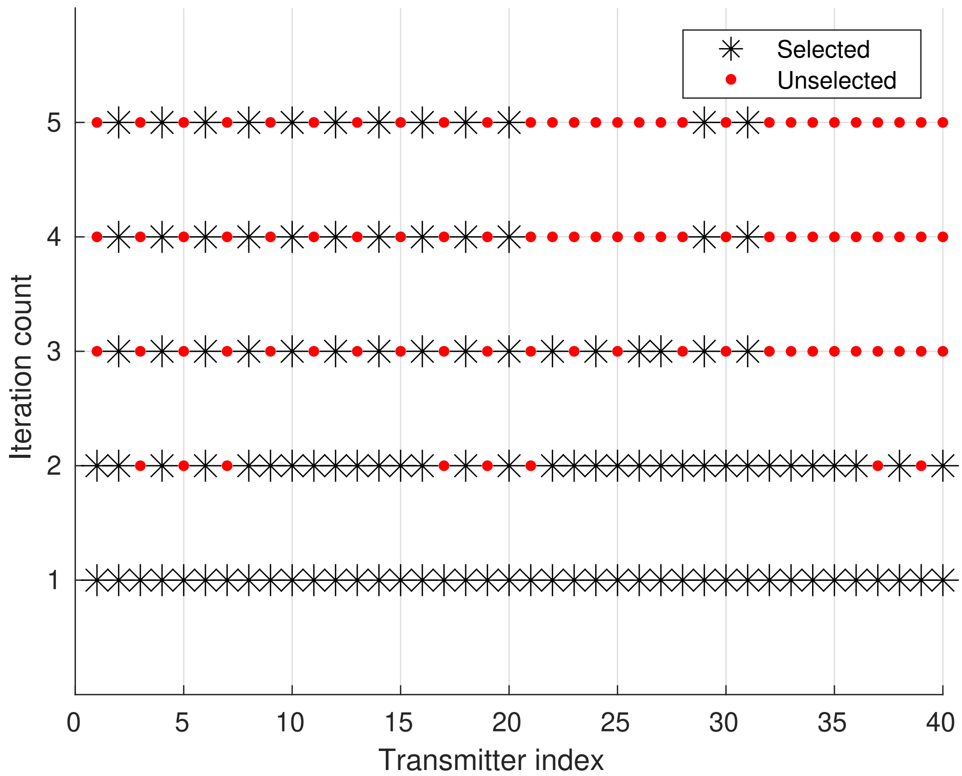

Figure 3.3. *Schematic of array profile for each iteration, showing the locations of selected antenna elements within the array with respect to their indices.*

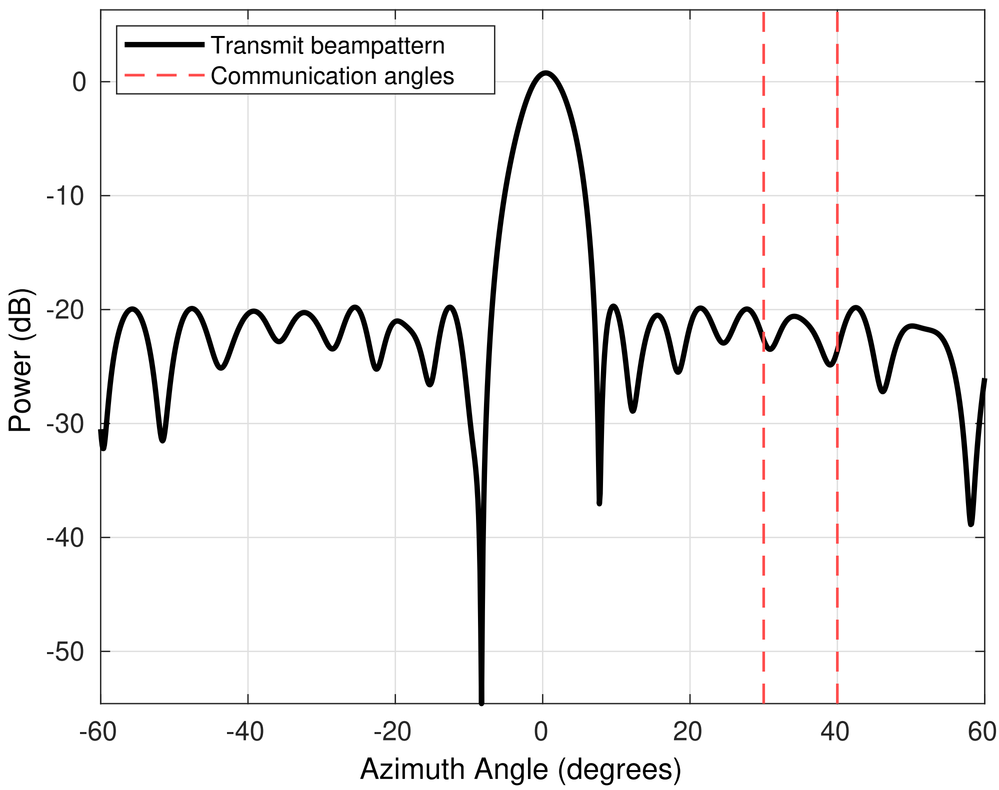

Figure 3.4. *Acquired antenna pattern after last iteration. Main beam length and position, along with the gain drop from main beam to sidelobes, are accurate to the given simulation settings.*

4. SCNR MAXIMIZATION STRATEGY FOR JRC SYSTEMS

This chapter provides a thorough explanation of finding the optimal beamformer for improving the detection performance in JRC systems by maximizing SCNR. Section 4.1 elaborates on how SCNR directly relates to detection performance of a radar system. System model is described along with signal model used for representing SCNR and SNR expressions for radar and communication operations, respectively, in section 4.2. A convex optimization problem is defined for maximizing radar SCNR while satisfying communications requirements in section 4.3, and a rank-reduction algorithm is applied in section 4.4 to convert the information acquired by solving the optimization problem into a weight vector that is usable in a beamforming system model. The chapter concludes with interpretation of simulation results in section 4.5.

4.1 Objective of SCNR Maximization

Analogous to the symbol detection in communication systems, radar systems rely on decision-making between two hypotheses of a target actually being present or not for detection. While the noise is always present in the system, the system receives a signal resulting from the reflections off the target in addition to noise in case of detection. Successfully distinguishing between the cases of a varying noise signal and a varying noise signal plus a varying target return signal relies on having a high SNR. Both the noise amplitude and target return signal amplitude have their own probability density functions (PDF) depending on noise PDF and transmit power, respectively. The probability of successfully identifying a case where detection occurs is referred to as the detection rate (DR), while the probability of making a decision in favour of detection while no target presence is named the false alarm rate (FAR). The detection threshold is negatively correlated with the FAR, alongside with the DR, which is positively correlated with peak output SNR in addition[41]. Besides the noise, clutter reflection is another source of FAR. Thus, in the radar system with the presence of clutter, the measurement signal-to-clutter-noise-ratio (SCNR) is often used for derive the DR. Thus, it necessarily follows from here that maximizing SCNR for a fixed FAR is equivalent to maximizing the DR, as shown in Figure 4.1.

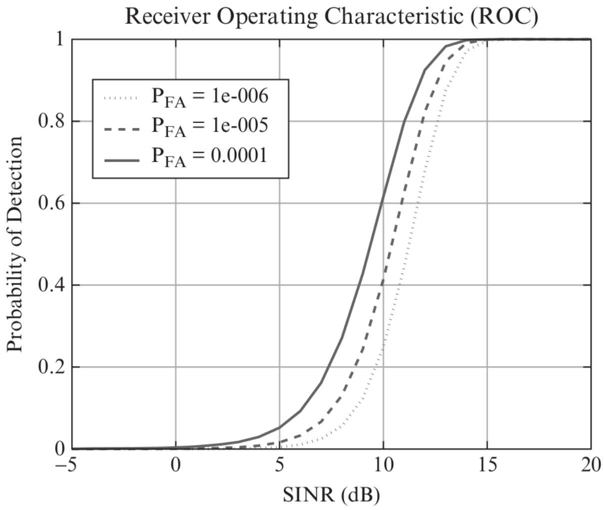

Figure 4.1. *Figure from [41] depicting the positive correlation between detection rate and signal-to-interference and noise ratio (SINR).*

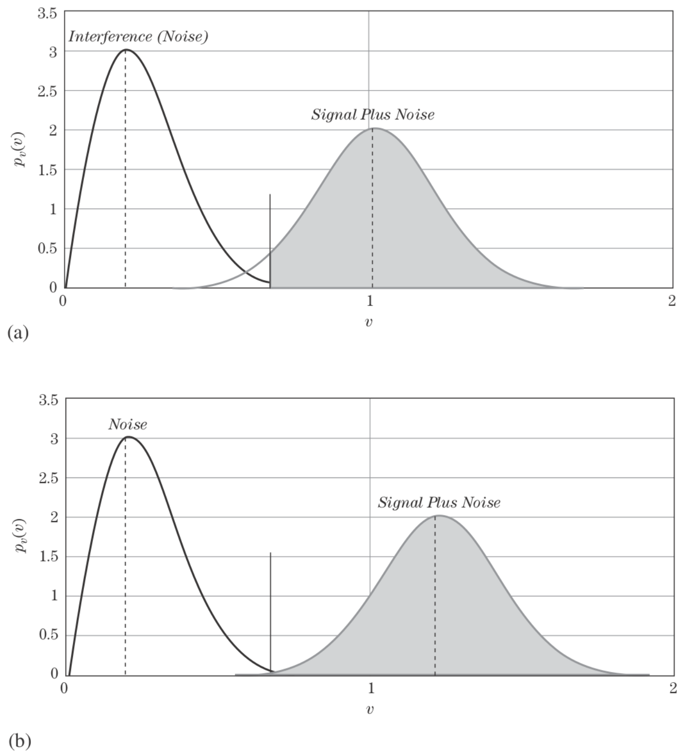

Figure 4.2. *Figure from [42] demonstrating the noise PDFs and target plus noise PDFs for lower and higher SNR cases in (a) and (b), respectively.*

A visual depiction of the relationship between detection rate and SNR is provided in Figure 4.2, where a smaller overlapping area exists between noise and target plus noise PDFs in higher SNR cases. SNR maximization is essential in the design of radar systems, and one of the optimum beamformers explained in Chapter 2.2.1 has maximization of SNR as its objective function. Even though that beamformer is generally suitable for radar applications, its expression for optimal weights is not directly usable in the JRC system model described in this chapter. There are extra constraints that emerge when radar and communication systems are merged, and they are critical for the JRC system performance. The multi-purpose system assumed in this work has to satisfy constraints for communication performance and power consumption in addition to maximizing the detection performance. The rest of this chapter elaborates on a method for maximizing the ratio of target return signal power to the noise power plus clutter return signal power combined, or signal to noise and clutter ratio (SCNR) for short, while satisfying the performance requirements for communication operation and power budget restriction at the same time for JRC system.

4.2 System model

The model used in this chapter is different from the one used in the previous chapter in terms of the system setting, assumed preliminary information about the system, and the mathematical expression used to state the optimization problem. The beamforming approach described in this part will be concerned with single-user mmWave JRC systems where there is only a single non-negligible clutter that can be detected by radar operation. A direct path for the communication operation is not assumed this time, and a channel vector $\boldsymbol{h}$ is used to model the reflectivities of possible point reflectors connecting the transmitter and user. Performance requirements for the communication operation are satisfied again by the problem constraints as the priority is still in the radar operation. However, this time, the constraints will enforce the communication performance by setting a lower threshold for SNR only. Direct connection is assumed between the transmitter and radar target along with clutter. Radar performance is ensured by setting the objective function as an expression proportional to the power transmitted to and received back from the direction of the target and inversely proportional to the added effects of the noise and power reflected back from clutter.

The system assumed in this part is a phased antenna array with half of the antennas allocated for transmitting the waveform that is used for both radar target detection and carrying the communication message, with the other half allocated for receiving the reflected signal from the radar target and clutter. The waveform is multiplied by the beamforming vector and put through a phase shifter before getting transmitted. Return signal sensed by the antenna elements allocated for receiving is subjected through the phase shifter again and processed further for the acquisition of sensing parameters which is beyond the scope of this work about beamforming. A schematic of the system setting can be seen in Figure 4.3.

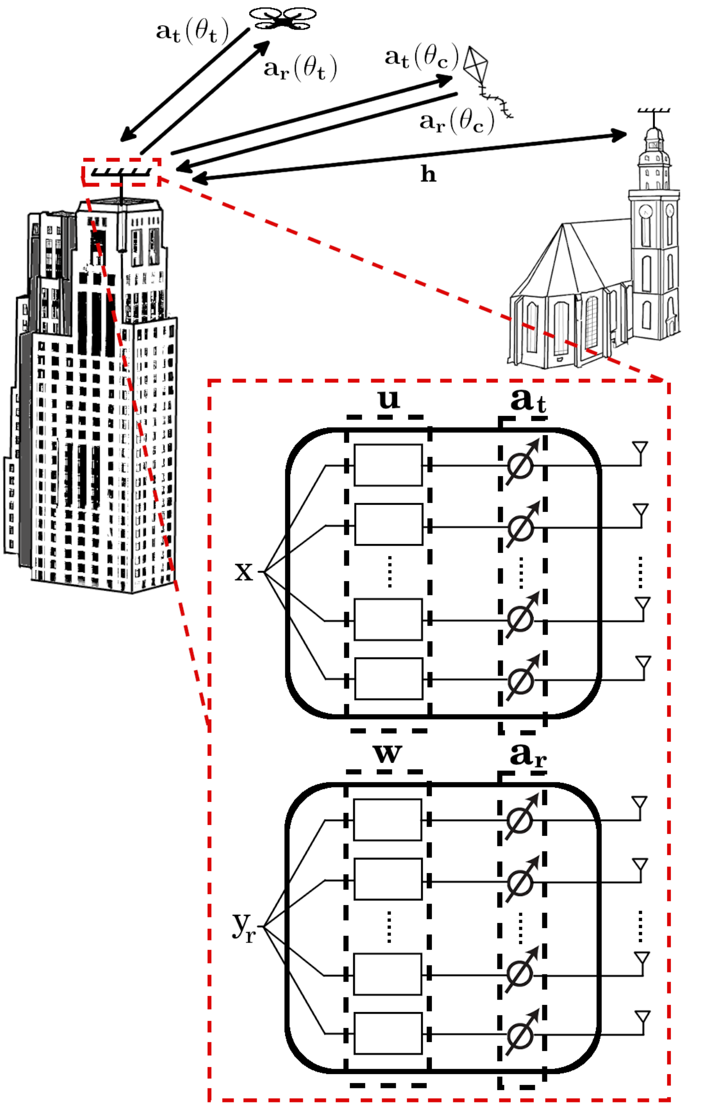

Figure 4.3. *Visualization of JRC operation and simplified block diagram of the transmitter side.*

The mathematical expression of the received radar signal is acquired by multiplying the transmit waveform x by weight vector $\boldsymbol{u}$, transmit and receive steering vectors $\boldsymbol{a}_t(\theta)$ and $\boldsymbol{a}_r(\theta)$ directed at radar target θ_t and clutter θ_c, scaled by reflection factors of the target σ_t and clutter σ_c:

$$\boldsymbol{r} = \sigma_t \boldsymbol{a}_r(\theta_t)\boldsymbol{a}_t^H(\theta_t)\boldsymbol{u}x + \sigma_c \boldsymbol{a}_r(\theta_c)\boldsymbol{a}_t^H(\theta_c)\boldsymbol{u}x + \boldsymbol{n}, \tag{4.1}$$

where $\boldsymbol{n}$ is the noise vector. Likewise, the signal received by the communication user is given by:

$$\boldsymbol{y}_c = \boldsymbol{h}^H \boldsymbol{u} x + \nu, \tag{4.2}$$

where ν is the noise affecting the transmitted communication symbol. Left multiplying (4.1) by $\boldsymbol{w}^H$ yields the received combined radar return signal, making the substitution $A(\theta) = \boldsymbol{a}_r(\theta)\boldsymbol{a}_t^H(\theta)$, it could be written as:

$$\boldsymbol{y}_r = \boldsymbol{w}^H \boldsymbol{r} = \sigma_t \boldsymbol{w}^H \boldsymbol{A}(\theta_t)\boldsymbol{u} x + \sigma_c \boldsymbol{w}^H \boldsymbol{A}(\theta_c)\boldsymbol{u} x + \boldsymbol{w}^H \boldsymbol{n}. \tag{4.3}$$

The average SCNR expression is acquired by the ratio of the target return signal power to the clutter return signal power plus noise power. Noise is assumed to have a variance of $N_0^{'}$ and thus could be shown as an identity matrix scaled by $N_0^{'}$:

$$\gamma_r = \frac{\sigma_t^2 |\boldsymbol{w}^H \boldsymbol{A}(\theta_t)\boldsymbol{u}|^2}{\sigma_c^2 \boldsymbol{w}^H (\boldsymbol{A}(\theta_c)\boldsymbol{u}\boldsymbol{u}^H \boldsymbol{A}^H(\theta_c) + \boldsymbol{I}\frac{N_0^{'}}{\sigma_c^2})\boldsymbol{w}}. \tag{4.4}$$

Average communication SNR is expressed similarly as:

$$\gamma_c = \frac{|\boldsymbol{h}^H \boldsymbol{u}|^2}{N_0^{'}}. \tag{4.5}$$

It is clear from (4.4), (4.5) that the radar SCNR and communication SNR are dependent on $\boldsymbol{u}$. In the next section, an optimization problem is formulated to find the optimal value of $\boldsymbol{u}$ which guarantees communication SNR over a set threshold while having the maximum possible radar SCNR.

4.3 Problem Formulation

Now those expressions will be used to form an optimization problem, and it will gradually be converted into a convex optimization problem. Maximizing γ_r by setting $\boldsymbol{w}$ and $\boldsymbol{u}$ vectors while keeping total transmit power $||\boldsymbol{u}||_2^2$ under an upper bound and keeping γ_c above a lower bound constitutes an optimization problem stated as:

$$\underset{\boldsymbol{w},\boldsymbol{u}}{\text{maximize}}\ \gamma_r = \sigma \frac{|\boldsymbol{w}^H \boldsymbol{A}(\theta_t)\boldsymbol{u}|^2}{\boldsymbol{w}^H (\boldsymbol{A}(\theta_c)\boldsymbol{u}\boldsymbol{u}^H \boldsymbol{A}^H(\theta_c) + \boldsymbol{I}N_0)\boldsymbol{w}} \tag{4.6}$$

$$\text{s. t.}\ \ ||\boldsymbol{u}||_2^2 \leq P_t, \tag{4.7}$$

$$\boldsymbol{w}^H \boldsymbol{w} = ||\boldsymbol{w}||_2^2 = 1, \tag{4.8}$$

$$\gamma_c = \frac{|\boldsymbol{h}^H \boldsymbol{u}|^2}{N_0^{'}} \geq \Gamma_c, \tag{4.9}$$

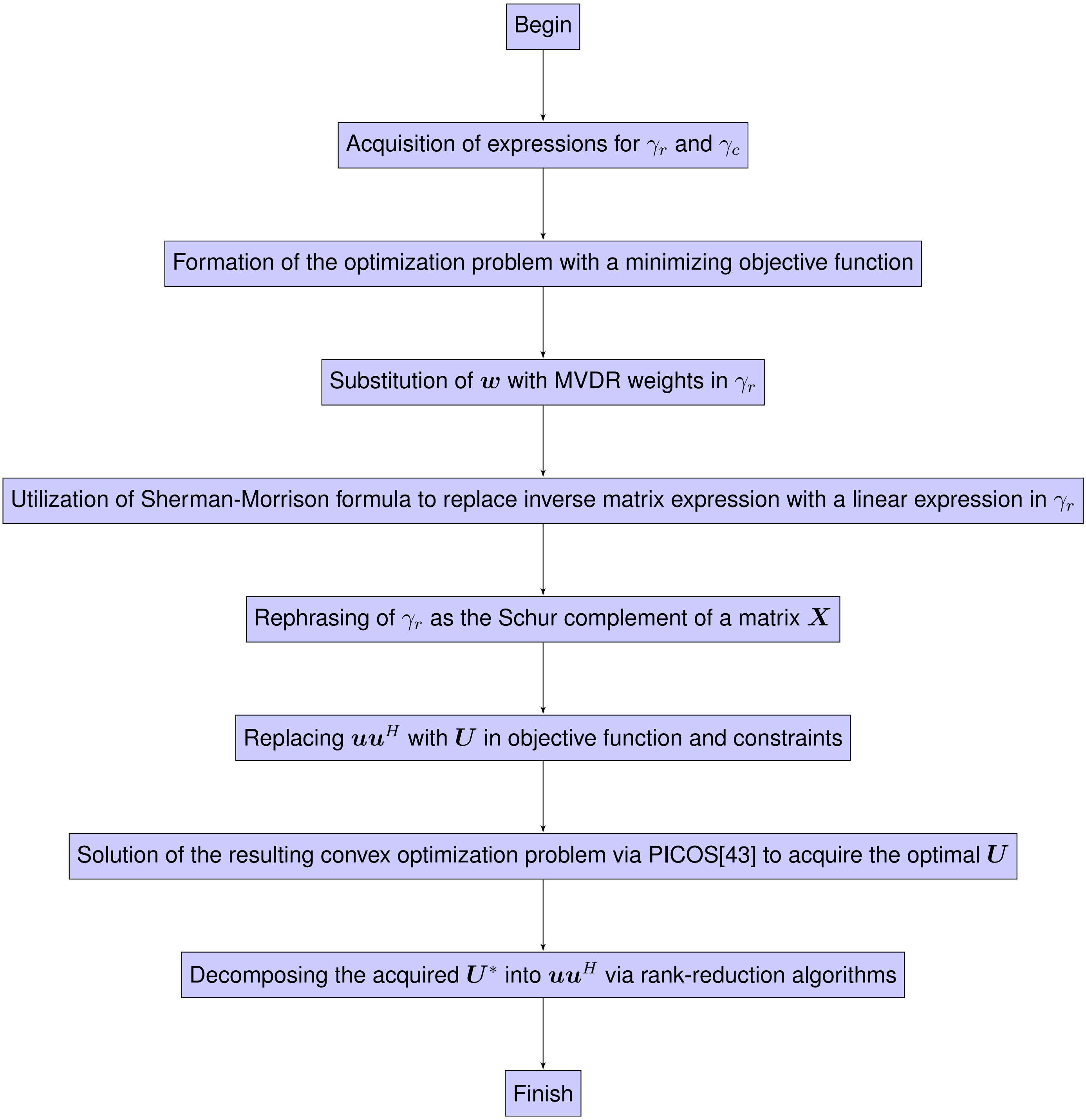

Figure 4.4. *Flowchart of the steps described in this chapter for acquiring the optimal beamforming weight vector $\mathbf{u}$ for maximizing radar SCNR.*

where $\sigma = \sigma_t^2/\sigma_c^2$ is the ratio between squares of target reflection factor and clutter reflection factor, and $N_0 = N_0'/\sigma_c^2$ is noise variance divided by squared clutter reflection factor. Receive weights $\boldsymbol{w}$ are expected to set gain for the radar target direction to unity while keeping the total array output power unchanged. Therefore, minimum variance distortionless response (MVDR) weights[44] can be used to express $\boldsymbol{w}$ in terms of $\boldsymbol{u}$ and $A(\theta)$.

$$\boldsymbol{w}_{MVDR} = \frac{\boldsymbol{M}^{-1}(\boldsymbol{u})\boldsymbol{A}(\theta_t)\boldsymbol{u}}{\boldsymbol{u}^H\boldsymbol{A}^H(\theta_t)\boldsymbol{M}^{-1}(\boldsymbol{u})\boldsymbol{A}(\theta_t)\boldsymbol{u}}, \tag{4.10}$$

where $\boldsymbol{M}$ is the spatial covariance matrix given by:

$$\boldsymbol{M}(\boldsymbol{u}) = \boldsymbol{A}(\theta_c)\boldsymbol{u}\boldsymbol{u}^H\boldsymbol{A}^H(\theta_c) + \boldsymbol{I}N_0 \tag{4.11}$$

Substituting $\boldsymbol{w}$ with $\boldsymbol{w}_{MVDR}$ in γ_r yields:

$$\gamma_r = \sigma\frac{|(\frac{\boldsymbol{M}^{-1}(\boldsymbol{u})\boldsymbol{A}(\theta_t)\boldsymbol{u}}{\boldsymbol{u}^H\boldsymbol{A}^H(\theta_t)\boldsymbol{M}^{-1}(\boldsymbol{u})\boldsymbol{A}(\theta_t)\boldsymbol{u}})^H\boldsymbol{A}(\theta_t)\boldsymbol{u}|^2}{(\frac{\boldsymbol{M}^{-1}(\boldsymbol{u})\boldsymbol{A}(\theta_t)\boldsymbol{u}}{\boldsymbol{u}^H\boldsymbol{A}^H(\theta_t)\boldsymbol{M}^{-1}(\boldsymbol{u})\boldsymbol{A}(\theta_t)\boldsymbol{u}})^H(\boldsymbol{A}^H(\theta_c)\boldsymbol{u}\boldsymbol{u}^H\boldsymbol{A}^H(\theta_c)+\boldsymbol{I}N_0)\frac{\boldsymbol{M}^{-1}(\boldsymbol{u})\boldsymbol{A}(\theta_t)\boldsymbol{u}}{\boldsymbol{u}^H\boldsymbol{A}^H(\theta_t)\boldsymbol{M}^{-1}(\boldsymbol{u})\boldsymbol{A}(\theta_t)\boldsymbol{u}}} \tag{4.12}$$

$$= \sigma\frac{(\frac{\boldsymbol{M}^{-1}(\boldsymbol{u})\boldsymbol{A}(\theta_t)\boldsymbol{u}}{\boldsymbol{u}^H\boldsymbol{A}^H(\theta_t)\boldsymbol{M}^{-1}(\boldsymbol{u})\boldsymbol{A}(\theta_t)\boldsymbol{u}})^H\boldsymbol{A}(\theta_t)\boldsymbol{u}\boldsymbol{u}^H\boldsymbol{A}^H(\theta_t)(\frac{\boldsymbol{u}^H\boldsymbol{A}(\theta_t)\boldsymbol{M}^{-1}(\boldsymbol{u})}{\boldsymbol{u}^H\boldsymbol{A}^H(\theta_t)\boldsymbol{M}^{-1}(\boldsymbol{u})\boldsymbol{A}(\theta_t)\boldsymbol{u}})}{(\frac{\boldsymbol{M}^{-1}(\boldsymbol{u})\boldsymbol{A}(\theta_t)\boldsymbol{u}}{\boldsymbol{u}^H\boldsymbol{A}^H(\theta_t)\boldsymbol{M}^{-1}(\boldsymbol{u})\boldsymbol{A}(\theta_t)\boldsymbol{u}})^H(\boldsymbol{A}^H(\theta_c)\boldsymbol{u}\boldsymbol{u}^H\boldsymbol{A}^H(\theta_c)+\boldsymbol{I}N_0)\frac{\boldsymbol{M}^{-1}(\boldsymbol{u})\boldsymbol{A}(\theta_t)\boldsymbol{u}}{\boldsymbol{u}^H\boldsymbol{A}^H(\theta_t)\boldsymbol{M}^{-1}(\boldsymbol{u})\boldsymbol{A}(\theta_t)\boldsymbol{u}}} \tag{4.13}$$

Since the value of $\boldsymbol{u}^H\boldsymbol{A}^H(\theta_t)\boldsymbol{M}^{-1}(\boldsymbol{u})\boldsymbol{A}(\theta_t)\boldsymbol{u}$ is a scalar and its multiplicative inverse is present in both numerator and denominator, it can directly be eliminated. That leads to:

$$\gamma_r = \sigma\frac{\boldsymbol{u}^H\boldsymbol{A}^H(\theta_t)\boldsymbol{M}^{-1}(\boldsymbol{u})\boldsymbol{A}(\theta_t)\boldsymbol{u}\boldsymbol{u}^H\boldsymbol{A}^H(\theta_t)\boldsymbol{M}^{-1}(\boldsymbol{u})\boldsymbol{A}(\theta_t)\boldsymbol{u}}{\boldsymbol{u}^H\boldsymbol{A}^H(\theta_t)\boldsymbol{M}^{-1}(\boldsymbol{u})(\boldsymbol{A}^H(\theta_c)\boldsymbol{u}\boldsymbol{u}^H\boldsymbol{A}^H(\theta_c)+\boldsymbol{I}N_0)\boldsymbol{M}^{-1}(\boldsymbol{u})\boldsymbol{A}(\theta_t)\boldsymbol{u}} \tag{4.14}$$

Multiplying both sides by the denominator after this elimination yields:

$$\begin{aligned}&\gamma_r\boldsymbol{u}^H\boldsymbol{A}^H(\theta_t)\boldsymbol{M}^{-1}(\boldsymbol{u})(\boldsymbol{A}^H(\theta_c)\boldsymbol{u}\boldsymbol{u}^H\boldsymbol{A}^H(\theta_c)+\boldsymbol{I}N_0)\boldsymbol{M}^{-1}(\boldsymbol{u})\boldsymbol{A}(\theta_t)\boldsymbol{u} = \dots\\&\sigma\boldsymbol{u}^H\boldsymbol{A}^H(\theta_t)\boldsymbol{M}^{-1}(\boldsymbol{u})\boldsymbol{A}(\theta_t)\boldsymbol{u}\boldsymbol{u}^H\boldsymbol{A}^H(\theta_t)\boldsymbol{M}^{-1}(\boldsymbol{u})\boldsymbol{A}(\theta_t)\boldsymbol{u}\end{aligned} \tag{4.15}$$

Both sides of the equation are multiplied with the vector $\boldsymbol{u}^H\boldsymbol{A}^H(\theta_t)\boldsymbol{M}^{-1}(\boldsymbol{u})$, so it is possible to eliminate it from both sides. Even though vectors do not have inverses themselves, they can be multiplied by their Hermitians to result in scalars or covariance matrices, which can be eliminated by getting multiplied by their multiplicative inverses. Eliminating the left-multiplied $\boldsymbol{u}^H\boldsymbol{A}^H(\theta_t)\boldsymbol{M}^{-1}(\boldsymbol{u})$ and right-multiplied by $\boldsymbol{M}^{-1}(\boldsymbol{u})\boldsymbol{A}(\theta_t)\boldsymbol{u}$ results in:

$$\gamma_r(\boldsymbol{A}^H(\theta_c)\boldsymbol{u}\boldsymbol{u}^H\boldsymbol{A}^H(\theta_c) + \boldsymbol{I}N_0) = \sigma\boldsymbol{A}(\theta_t)\boldsymbol{u}\boldsymbol{u}^H\boldsymbol{A}^H(\theta_t) \tag{4.16}$$

$$\gamma_r\boldsymbol{M}(\boldsymbol{u}) = \sigma\boldsymbol{A}(\theta_t)\boldsymbol{u}\boldsymbol{u}^H\boldsymbol{A}^H(\theta_t) \tag{4.17}$$

Right-multiplying both sides with $\boldsymbol{M}^{-1}(\boldsymbol{u})\boldsymbol{A}(\theta_t)\boldsymbol{u}$ results in:

$$\gamma_r\boldsymbol{A}(\theta_t)\boldsymbol{u} = \sigma\boldsymbol{A}(\theta_t)\boldsymbol{u}\boldsymbol{u}^H\boldsymbol{A}^H(\theta_t)\boldsymbol{M}^{-1}(\boldsymbol{u})\boldsymbol{A}(\theta_t)\boldsymbol{u} \tag{4.18}$$

Now both sides can be left-multiplied first by $\boldsymbol{u}^H\boldsymbol{A}^H(\theta_t)$, then by $(\boldsymbol{u}^H\boldsymbol{A}^H(\theta_t)\boldsymbol{A}(\theta_t)\boldsymbol{u})^{-1}$ in order to eliminate the $\boldsymbol{A}(\theta_t)\boldsymbol{u}$ expression from both sides. This allows the problem statement to be rewritten as:

$$\underset{\boldsymbol{u}}{\text{maximize}}\ \gamma_r = \sigma\boldsymbol{u}^H\boldsymbol{A}^H(\theta_t)\boldsymbol{M}^{-1}(\boldsymbol{u})\boldsymbol{A}(\theta_t)\boldsymbol{u} \tag{4.19}$$

$$\text{s. t.}\ \ ||\boldsymbol{u}||_2^2 \leq P_t, \tag{4.20}$$

$$\gamma_c = \frac{|\boldsymbol{h}^H\boldsymbol{u}|^2}{N_0'} \geq \Gamma_c \tag{4.21}$$

Then this problem can be rephrased so that the objective function is a minimum:

$$\underset{\boldsymbol{u}}{\text{minimize}}\ -y \tag{4.22}$$

$$\text{s. t.}\ \ \sigma\boldsymbol{u}^H\boldsymbol{A}^H(\theta_t)\boldsymbol{M}^{-1}(\boldsymbol{u})\boldsymbol{A}(\theta_t)\boldsymbol{u} \geq y \tag{4.23}$$

$$||\boldsymbol{u}||_2^2 \leq P_t, \tag{4.24}$$

$$\gamma_c = \frac{|\boldsymbol{h}^H\boldsymbol{u}|^2}{N_0'} \geq \Gamma_c \tag{4.25}$$

The inverse matrix expression $\boldsymbol{M}^{-1}(\boldsymbol{u})$ can be converted to a linear expression by utilizing Sherman-Morrison formula[45]:

$$(\boldsymbol{N} + \boldsymbol{a}\boldsymbol{b}^T)^{-1} = \boldsymbol{N}^{-1} - \frac{\boldsymbol{N}^{-1}\boldsymbol{a}\boldsymbol{b}^T\boldsymbol{N}^{-1}}{1 + \boldsymbol{b}^T\boldsymbol{N}^{-1}\boldsymbol{a}} \tag{4.26}$$

where $\boldsymbol{N} \in \mathbb{R}^{n\times n}$ is an invertible square matrix and $\boldsymbol{b}, \boldsymbol{a} \in \mathbb{R}^n$ are column vectors, and $1 + \boldsymbol{b}^T\boldsymbol{N}^{-1}\boldsymbol{a} \neq 0$. $\boldsymbol{N}$ is an identity matrix scaled by N_0 in the case of this problem, and

$\boldsymbol{a} = \boldsymbol{b} = \boldsymbol{A}(\theta_c)\boldsymbol{u}$. Substituting those in the formula yields:

$$\boldsymbol{M}^{-1}(\boldsymbol{u}) = (\boldsymbol{I}N_0 + \boldsymbol{A}(\theta_c)\boldsymbol{u}\boldsymbol{u}^H\boldsymbol{A}^H(\theta_c))^{-1} \tag{4.27}$$

$$= \boldsymbol{I}\frac{1}{N_0} - \frac{\frac{1}{N_0}\boldsymbol{I}\boldsymbol{A}(\theta_c)\boldsymbol{u}\boldsymbol{u}^H\boldsymbol{A}^H(\theta_c)\frac{1}{N_0}\boldsymbol{I}}{1 + \boldsymbol{u}^H\boldsymbol{A}^H(\theta_c)\frac{1}{N_0}\boldsymbol{I}\boldsymbol{A}(\theta_c)} \tag{4.28}$$

$$= \frac{1}{N_0}(\boldsymbol{I} - \frac{\boldsymbol{A}(\theta_c)\boldsymbol{u}\boldsymbol{u}^H\boldsymbol{A}^H(\theta_c)}{N_0 + \boldsymbol{u}^H\boldsymbol{A}^H(\theta_c)\boldsymbol{A}(\theta_c)\boldsymbol{u}}) \tag{4.29}$$

$$= \frac{1}{N_0}(\boldsymbol{I} - \frac{\boldsymbol{A}(\theta_c)\boldsymbol{u}\boldsymbol{u}^H\boldsymbol{A}^H(\theta_c)}{N_0 + tr(\boldsymbol{A}(\theta_c)\boldsymbol{u}\boldsymbol{u}^H\boldsymbol{A}^H(\theta_c))}) \tag{4.30}$$

Substituting this with $\boldsymbol{M}^{-1}$ in the γ_r expression yields:

$$\gamma_r = \frac{\sigma}{N_0}\boldsymbol{u}^H\boldsymbol{A}^H(\theta_t)(\boldsymbol{I} - \frac{\boldsymbol{A}(\theta_c)\boldsymbol{u}\boldsymbol{u}^H\boldsymbol{A}^H(\theta_c)}{N_0 + tr(\boldsymbol{A}(\theta_c)\boldsymbol{u}\boldsymbol{u}^H\boldsymbol{A}^H(\theta_c))})\boldsymbol{A}(\theta_t)\boldsymbol{u}. \tag{4.31}$$

Expression in (4.23) can be rewritten as $\gamma_r - y \geq 0$ in order to treat $\gamma_r - y$ as a 1×1 positive semi-definite matrix and utilize Schur complement to further transform the problem. Let a matrix $\boldsymbol{X}$ be defined such that:

$$\boldsymbol{X} = \begin{bmatrix} \boldsymbol{A}(\boldsymbol{u}\boldsymbol{u}^H) & \boldsymbol{B}(\boldsymbol{u}\boldsymbol{u}^H) \\ \boldsymbol{B}^H(\boldsymbol{u}\boldsymbol{u}^H) & \boldsymbol{C}(\boldsymbol{u}\boldsymbol{u}^H) \end{bmatrix}, \tag{4.32}$$

where,

$$\boldsymbol{A}(\boldsymbol{u}\boldsymbol{u}^H) = \frac{\sigma}{N_0}\boldsymbol{u}^H\boldsymbol{A}^H(\theta_t)\boldsymbol{A}(\theta_t)\boldsymbol{u} - y, \tag{4.33}$$

$$= \frac{tr(\boldsymbol{A}(\theta_t)\boldsymbol{u}\boldsymbol{u}^H\boldsymbol{A}^H(\theta_t))}{N_0} - y,$$

$$\boldsymbol{B}(\boldsymbol{u}\boldsymbol{u}^H) = \boldsymbol{u}^H\boldsymbol{A}^H(\theta_t)\boldsymbol{A}(\theta_c)\boldsymbol{u}, \tag{4.34}$$

$$= tr(\boldsymbol{A}(\theta_c)\boldsymbol{u}\boldsymbol{u}^H\boldsymbol{A}^H(\theta_t)),$$

$$\boldsymbol{B}(\boldsymbol{u}\boldsymbol{u}^H)^H = \boldsymbol{u}^H\boldsymbol{A}^H(\theta_c)\boldsymbol{A}(\theta_t)\boldsymbol{u}, \tag{4.35}$$

$$= tr(\boldsymbol{A}(\theta_t)\boldsymbol{u}\boldsymbol{u}^H\boldsymbol{A}^H(\theta_c)),$$

$$\boldsymbol{C}(\boldsymbol{u}\boldsymbol{u}^H) = \frac{N_0}{\sigma}(N_0 + tr(\boldsymbol{A}(\theta_c)\boldsymbol{u}\boldsymbol{u}^H\boldsymbol{A}^H(\theta_c))). \tag{4.36}$$

It should be minded that since expressions for $\boldsymbol{A}$, $\boldsymbol{B}$, and $\boldsymbol{C}$ all result in scalars when evaluated, they can be put in trace operations without their values getting changed. They can then get reorganized inside trace operation due to the cyclic property of trace: $tr(\boldsymbol{ABC}) = tr(\boldsymbol{BCA}) = tr(\boldsymbol{CAB})$.

According to Schur complement's conditions for positive definiteness semi-definiteness, provided that $\boldsymbol{C}$ is positive definite, then $\boldsymbol{X}$ is positive semi-definite if and only if its Schur complement $\boldsymbol{X}/\boldsymbol{C}$ is positive semi-definite[46].

$$\text{If } \boldsymbol{C} \succ 0, \text{ then } \boldsymbol{X} \succeq 0 \Leftrightarrow \boldsymbol{X}/\boldsymbol{C} = \boldsymbol{A} - \boldsymbol{B}\boldsymbol{C}^{-1}\boldsymbol{B}^H \succeq 0. \tag{4.37}$$

$\boldsymbol{C}(\boldsymbol{u}\boldsymbol{u}^H)$ is clearly positive definite since it is an expression of addition of two non-zero real numbers. Positive semi-definiteness of one of $\boldsymbol{X}/\boldsymbol{C}$ or $\boldsymbol{X}$ imply the positive semi-definiteness of the other, and $\boldsymbol{X}/\boldsymbol{C}$ is equal to:

$$\boldsymbol{X}/\boldsymbol{C} = \boldsymbol{A} - \boldsymbol{B}\boldsymbol{C}^{-1}\boldsymbol{B}^H, \tag{4.38}$$

$$= \frac{\sigma}{N_0}\boldsymbol{u}^H\boldsymbol{A}^H(\theta_t)\boldsymbol{A}(\theta_t)\boldsymbol{u} - y - \frac{\boldsymbol{u}^H\boldsymbol{A}^H(\theta_t)\boldsymbol{A}(\theta_c)\boldsymbol{u}\boldsymbol{u}^H\boldsymbol{A}^H(\theta_c)\boldsymbol{A}(\theta_t)\boldsymbol{u}}{\frac{N_0}{\sigma}(N_0 + tr(\boldsymbol{A}(\theta_c)\boldsymbol{u}\boldsymbol{u}^H\boldsymbol{A}^H(\theta_c)))}, \tag{4.39}$$

$$= \frac{\sigma}{N_0}\boldsymbol{u}^H\boldsymbol{A}^H(\theta_t)(\boldsymbol{I} - \frac{\boldsymbol{A}(\theta_c)\boldsymbol{u}\boldsymbol{u}^H\boldsymbol{A}^H(\theta_c)}{N_0 + tr(\boldsymbol{A}(\theta_c)\boldsymbol{u}\boldsymbol{u}^H\boldsymbol{A}^H(\theta_c))})\boldsymbol{A}(\theta_t)\boldsymbol{u} - y, \tag{4.40}$$

$$= \gamma_r - y. \tag{4.41}$$

Since $\gamma_r - y$ is equal to $\boldsymbol{X}/\boldsymbol{C}$ and it being larger than or equal to 0 implies the positive semi-definiteness of X and vice versa, the optimization problem constraint involving γ_r and y can be rewritten as a constraint enforcing the positive semi-definiteness of X,

$$\underset{\boldsymbol{u}}{\text{minimize}} \;\; -y \tag{4.42}$$

$$\text{s. t.} \;\; \boldsymbol{X} \succeq 0, \tag{4.43}$$

$$||\boldsymbol{u}||_2^2 \leq P_t, \tag{4.44}$$

$$\gamma_c = \frac{|\boldsymbol{h}^H\boldsymbol{u}|^2}{N_0'} \geq \Gamma_c, \tag{4.45}$$

where $\boldsymbol{X}$ is the matrix described in (4.32). One last factor that keeps this problem from being convex is that expression $\boldsymbol{u}\boldsymbol{u}^H$ which can be written as $\boldsymbol{U}$ in order to get rid of the quadratic expression. It is also required to change the other expressions with $\boldsymbol{u}\boldsymbol{u}^H$ in the problem statement to equivalent statements with $\boldsymbol{U}$ for the sake of convexity. Constraint of power budget, $||\boldsymbol{u}||_2^2 \leq P_t$ can also be rewritten as $tr(\boldsymbol{U}) \leq P_t$ by the steps:

$$||\boldsymbol{u}||_2^2 = \boldsymbol{u}^H\boldsymbol{u} \qquad \text{Sum of each vector element's square} \tag{4.46}$$

$$= tr(\boldsymbol{u}^H\boldsymbol{u}) \qquad \text{Trace of a scalar is equal to that scalar itself} \tag{4.47}$$

$$= tr(\boldsymbol{u}\boldsymbol{u}^H) \qquad \text{Cyclic property of trace} \tag{4.48}$$

$$= tr(\boldsymbol{U}) \tag{4.49}$$

Likewise, problem constraint enforcing the lower threshold for communication operation

SNR can be rewritten as an expression of $\boldsymbol{U}$ by applying these steps on γ_c:

$$\gamma_c = \frac{|\boldsymbol{h}^H \boldsymbol{u}|^2}{N_0'} \quad \text{Squared magnitude of a complex scalar} \tag{4.50}$$

$$= \frac{\boldsymbol{h}^H \boldsymbol{u}\boldsymbol{u}^H \boldsymbol{h}}{N_0'} \quad \text{Equal to multiplying the scalar with its complex conjugate} \tag{4.51}$$

$$= \frac{tr(\boldsymbol{h}^H \boldsymbol{u}\boldsymbol{u}^H \boldsymbol{h})}{N_0'} \quad \text{Trace of a scalar is equal to that scalar itself} \tag{4.52}$$

$$= \frac{tr(\boldsymbol{h}\boldsymbol{h}^H \boldsymbol{u}\boldsymbol{u}^H)}{N_0'} \quad \text{Cyclic property of trace} \tag{4.53}$$

$$= \frac{tr(\boldsymbol{U}\boldsymbol{H})}{N_0'} \quad \boldsymbol{h}\boldsymbol{h}^H \text{ is written as } \boldsymbol{H} \tag{4.54}$$

Replacing all of these expressions with their counterparts in the original problem statement results in:

$$\underset{\boldsymbol{U}}{\text{minimize}} \; -y \tag{4.55}$$

$$\text{s. t.} \quad \boldsymbol{X} = \begin{bmatrix} \boldsymbol{A}(\boldsymbol{U}) & \boldsymbol{B}(\boldsymbol{U}) \\ \boldsymbol{B}^H(\boldsymbol{U}) & \boldsymbol{C}(\boldsymbol{U}) \end{bmatrix} \succeq 0, \tag{4.56}$$

$$tr(\boldsymbol{U}) \leq P_t, \tag{4.57}$$

$$\gamma_c = \frac{tr(\boldsymbol{U}\boldsymbol{H})}{N_0'} \geq \Gamma_c. \tag{4.58}$$

(4.59)

$\boldsymbol{U}$ is acquired by the multiplication of $\boldsymbol{u}$ by its Hermitian. It is possible to enforce the property of $\boldsymbol{U}$ being a Hermitian matrix by defining it as such in the solver tool. However, it is also required to express that $\boldsymbol{U}$ should only have one vector spanning its range. Adding the constraint $rank(\boldsymbol{U}) = 1$ would satisfy that requirement, but it will also render the problem unsolvable by complex optimization algorithms since rank constraints are non-convex expressions. A suitable approach here is to solve the stated problem without imposing any constraints on the rank of $\boldsymbol{U}$ and then process the resulting $\boldsymbol{U}$ through a rank-reduction algorithm in order to get a rank one matrix that can be decomposed as $\boldsymbol{U} = \boldsymbol{u}\boldsymbol{u}^H$ where $\boldsymbol{u}$ will be the weight vector to be used in beamforming as shown in Figure 4.3.

4.4 Rank reduction

Inputting the previous problem statement through a convex optimization problem solver tool results in the minimum possible value of y, and values of $\boldsymbol{U}$, $\boldsymbol{X}$, γ_c that provide the satisfaction of conditions for acquiring that result. Let the values acquired from the problem solution represented with an asterisk such as $\boldsymbol{U}^*$. The elements of matrix $\boldsymbol{X}$ with solved values can be shown as:

$$\boldsymbol{X} = \begin{bmatrix} \frac{\sigma}{N_0} tr(\boldsymbol{A}(\theta_t)\boldsymbol{U}^*\boldsymbol{A}^H(\theta_t)) - y^* & tr(\boldsymbol{A}(\theta_c)\boldsymbol{U}^*\boldsymbol{A}^H(\theta_t)) \\ tr(\boldsymbol{A}(\theta_t)\boldsymbol{U}^*\boldsymbol{A}^H(\theta_c)) & \frac{N_0}{\sigma}(N_0 + tr(\boldsymbol{A}(\theta_c)\boldsymbol{U}^*\boldsymbol{A}^H(\theta_c))) \end{bmatrix} = \begin{bmatrix} a^* & b^* \\ b^* & c^* \end{bmatrix}. \tag{4.60}$$

Here it should be noted that two elements of matrix $\boldsymbol{X}$, $\boldsymbol{B}(\boldsymbol{U})$ and $\boldsymbol{B}^H(\boldsymbol{U})$ are equivalent to each other due to a property of trace operation:

$$tr(\boldsymbol{M}^H) = tr(\boldsymbol{M}) \qquad \text{For any matrix } \boldsymbol{M} \tag{4.61}$$

$$tr((\boldsymbol{A}(\theta_c)\boldsymbol{U}^*\boldsymbol{A}^H(\theta_t))^H) = tr(\boldsymbol{A}(\theta_t)\boldsymbol{U}^*\boldsymbol{A}^H(\theta_c)) = b^* \tag{4.62}$$

Writing the expressions for elements of $\boldsymbol{X}$ in open form, isolating the operations involving $\boldsymbol{U}^*$, and rearranging the trace operation inputs by cyclic property results in:

$$tr(\boldsymbol{A}^H(\theta_t)\boldsymbol{A}(\theta_t)\boldsymbol{U}^*) = \frac{N_0}{\sigma}(a^* + y^*) \tag{4.63}$$

$$tr(\boldsymbol{A}^H(\theta_t)\boldsymbol{A}(\theta_c)\boldsymbol{U}^*) = tr(\boldsymbol{A}^H(\theta_c)\boldsymbol{A}(\theta_t)\boldsymbol{U}^*) = b^* \tag{4.64}$$

$$tr(\boldsymbol{A}^H(\theta_c)\boldsymbol{A}(\theta_c)\boldsymbol{U}^*) = \frac{\sigma}{N_0}(c^* - N_0) \tag{4.65}$$

Additionally, there are two more equations relating $\boldsymbol{U}^*$ to other values acquired by optimization problem solution.

$$tr(\boldsymbol{U}^*) = P^* \tag{4.66}$$

$$tr(\boldsymbol{U}^*\boldsymbol{H}) = \gamma_c^* N_0' \tag{4.67}$$

Now the task of performing the rank one decomposition $\boldsymbol{U}^* = \boldsymbol{u}\boldsymbol{u}^H$ is equivalent to finding a vector $\boldsymbol{u}$ that satisfies the equations (4.63) to (4.67) when $\boldsymbol{U}^*$ is substituted by $\boldsymbol{u}\boldsymbol{u}^H$ in those. Among these equations, (4.64) could be eliminated by approximating $\boldsymbol{A}^H(\theta_t)\boldsymbol{A}(\theta_c)$ as 0. This is due to the fact that steering vectors directed to different angles approach to orthogonality with each other as the number of antennas approaches infinity, as stated in Corollary 2 in [47]. Since this approximation describes an equation where $\boldsymbol{U}^*$ is multiplied by zero, which will be satisfied as $b^* = 0$ no matter the value of $\boldsymbol{U}^*$, there are only 4 non-trivial equations that define $\boldsymbol{u}$.

Current problem is to find a vector $\boldsymbol{u}$ such that:

$$tr(\boldsymbol{A}^H(\theta_t)\boldsymbol{A}(\theta_t)\boldsymbol{u}\boldsymbol{u}^H) = tr(\boldsymbol{A}^H(\theta_t)\boldsymbol{A}(\theta_t)\boldsymbol{U}^*) = \frac{N_0}{\sigma}(a^* + y^*), \tag{4.68}$$

$$tr(\boldsymbol{A}^H(\theta_c)\boldsymbol{A}(\theta_c)\boldsymbol{u}\boldsymbol{u}^H) = tr(\boldsymbol{A}^H(\theta_t)\boldsymbol{A}(\theta_c)\boldsymbol{U}^*) = \frac{\sigma}{N_0}c^* - N_0, \tag{4.69}$$

$$tr(\boldsymbol{u}\boldsymbol{u}^H) = tr(\boldsymbol{U}^*) = P^*, \tag{4.70}$$

$$tr(\boldsymbol{u}\boldsymbol{u}^H\boldsymbol{H}) = tr(\boldsymbol{U}^*\boldsymbol{H}) = \gamma_c^* N_0'. \tag{4.71}$$

Now in order to acquire the optimal beamforming vector $\boldsymbol{u}$, it is needed to apply the Theorem 2.3 in [48], which relies on previously established theorems [49][50]. Theorem assumes four Hermitian matrices, A_1, A_2, A_3 and A_4, of size n where $n \geq 3$, and another Hermitian matrix of the same size, X, that has rank r and is positive semidefinite. It further assumes that at least one matrix among A_1, A_2, A_3 and A_4 has a nonzero result when put through inner product operation, $A \bullet Y = Re\{tr(A^H Y)\}$, with any nonzero Hermitian positive semidefinite matrix Y of size n. The theorem states that one can find a nonzero vector y such that:

$$A_1 \bullet \boldsymbol{y}\boldsymbol{y}^H = A_1 \bullet X \tag{4.72}$$

$$A_2 \bullet \boldsymbol{y}\boldsymbol{y}^H = A_2 \bullet X \tag{4.73}$$

$$A_3 \bullet \boldsymbol{y}\boldsymbol{y}^H = A_3 \bullet X \tag{4.74}$$

$$A_4 \bullet \boldsymbol{y}\boldsymbol{y}^H = A_4 \bullet X \tag{4.75}$$

where $y \in Range(X)$ if $r \geq 3$. If $r = 2$, then for any $z \notin Range(X)$ y exists in the linear subspace spanned by z and $Range(X)$. This can be applied to the problem discussed in this chapter by making the substitutions $A_1 = \boldsymbol{A}^H(\theta_t)\boldsymbol{A}(\theta_t)$, $A_2 = \boldsymbol{A}^H(\theta_c)\boldsymbol{A}(\theta_c)$, $A_3 = \boldsymbol{I}$, $A_4 = \boldsymbol{H}$, and $X = \boldsymbol{U}^*$. Further elaboration on the algorithm for acquiring $\boldsymbol{y}$ has been done in Appendix A. The resulting vector $\boldsymbol{y}$ will be the optimal beamforming vector represented with $\boldsymbol{u}$ until now.

4.5 Simulation Results

Simulations aimed to observe the tradeoff between performances of radar and communication operations were performed on situations with varying antenna array elements and lower thresholds for communication operation SNR. PICOS[43] was used as the tool for solving optimization problems in this chapter. Parameters for the noise power and transmit power had the most critical effect on the system performance due to their ratios to each other being directly related to SCNR. In the simulations whose results are presented in this subsection, ratio of transmit power to the noise power was set as 100. Constant values of clutter and target reflection factors were set as $\sigma_c = \sigma_t = 1$ during the simulations. Direction of the target was set towards $30°$, while clutter direction was set as $60°$. Distance between antenna elements was assumed to be $d = \lambda/2$ when modelling steering vectors $\boldsymbol{a}_t(\theta)$ and $\boldsymbol{a}_r(\theta)$, where λ is the transmit signal wavelength. The convex optimization problem for each and every one of the situations was solved with a new randomized channel vector for each iteration before performing the rank reduction to acquire the $\boldsymbol{u}$ vector for each case. Simulations were repeated 20 times with different randomly generated channel vectors every time, and resulting values of radar SCNR and communication SNR were averaged over all 20 results.

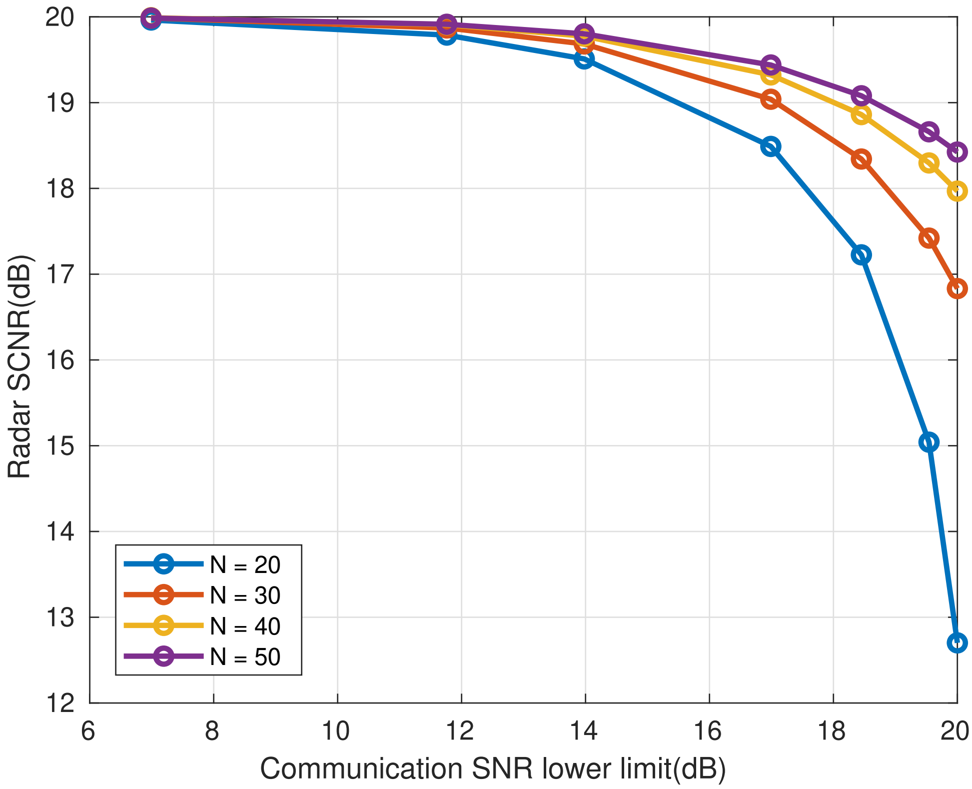

Figure 4.5. *Change in radar SCNR as different values of communication SNR are ensured by setting different Γ_c values ranging from 7 dB to 20 dB when defining problem constraints. N is the number of antennas.*

Expected trends of inversely related radar SCNR and communication SNR, in addition to better radar SCNR with a larger number of antennas, can clearly be observed from Figure 4.5. It should be noted that radar SCNR values here are not actual values calculated by the radar range equation, but rather are range-independent values calculated from equation (4.31) that give a measure that is proportional to the actual SCNR value for comparison purposes. Change in performance based on target distance is not in the scope of this work, but actual values can be estimated from the ones acquired from simulation since radar SCNR is inversely proportional to target range to the power of 4.

Another set of simulations was performed for the purpose of inspecting how the approximation made about b^* in previous subsection affected the results. It was possible to find the vector $\boldsymbol{u}$ resulting in a matrix that is approximately equivalent to $\boldsymbol{U}^*$ when multiplied by its Hermitian, since there were 4 equations defining $\boldsymbol{U}^*$ was described from (4.68) to (4.71). This was, however, only possible due to ignoring a fifth equation that related b^* to $\boldsymbol{U}^*$. Even though it is theoretically known that steering vectors directed at different angles are orthogonal to each other as the number of antenna elements approaches infinity, there will obviously be a smaller number of antenna elements in real applications. This results in $\boldsymbol{u}\boldsymbol{u}^*$ producing a different result than $\boldsymbol{U}^*$ would produce when substituted for it in (4.64). This implies that $\boldsymbol{u}$ is slightly different than the optimal possible vector, and the difference is expected to get smaller as the number of antennas increases. An extra pair of conditions, $tr(\boldsymbol{A}^H(\theta_t)\boldsymbol{A}(\theta_c)\boldsymbol{U}^*) = 0$, and $tr(\boldsymbol{A}^H(\theta_c)\boldsymbol{A}(\theta_t)\boldsymbol{U}^*) = 0$ were added to the optimization problem to enforce b^* actually being equal to 0. Results acquired from

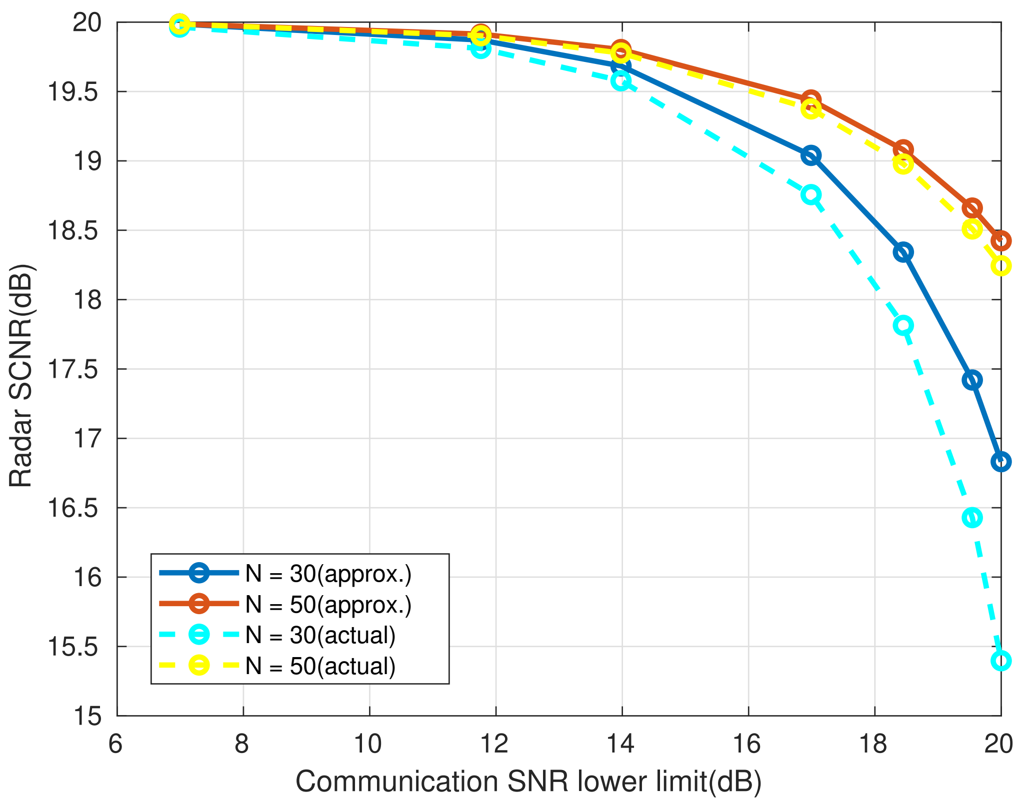

Figure 4.6. *Radar SCNR versus communication SNR plots with the different number of antenna elements, for cases where b^* is approximated to be zero and for cases where b^* is actually zero.*

simulations that had these constraints in their convex optimization phase were indicating lower performance than results that did not have those constraints, which is expected since adding more conditions leads to a lower maximum or higher minimum in optimization problems, and the difference between those results was observed to be smaller for cases with the higher number of antenna elements as seen in Figure 4.6. This is due to the fact that b^* is already quite close to 0 for a large number of antennas, and extra conditions do not put any serious restriction on the problem that would cause a non-negligible change in the optimal result.

5. CONCLUSION

This thesis work investigates optimal beamforming in joint radar and communication systems. The main contribution is the novel SCNR maximization method for JRC systems with no direct path between communication users, presented in Chapter 4. Other contributions and conclusions include reviews of previous works about joint radar and communication systems, particularly on antenna selection and beamforming. A mathematically intensive approach was followed during the writing phase and the viability of the proposed methods was shown theoretically. Chapter by chapter conclusions are as follows:

Preliminary work for this thesis was based on reviewing and duplicating the antenna selection algorithm proposed in [6], and Chapter 3 is devoted to that. The system model is shortly described as a JRC system that utilizes QAM-based sidelobe modulation. The motivation behind devising an antenna selection algorithm is explained, which could be summarized as reducing the number of costly RF chains used for the JRC operation via connecting multiple transmit antennas for each RF chain and using the smallest number of antennas among those for the JRC operation. In contrast, the rest are used for other possible operations simultaneously. The objective function is stated with respect to a reference main beam pattern similar to the reference signal beamformer. The direct path between communication users was assumed in the system model. Then norm functions are shortly explained since l_0 norms and approximating them by calculating iteratively weighted l_1 norms constitute a core point of the antenna selection algorithm. The initial algorithm that optimizes the transmit power and antenna selection while satisfying the system constraints for a single instance of communication transmission is presented. Even though this algorithm satisfies the optimization goals for a single scenario, transmit symbols change during transmission in practice, and this requires beamforming weights to be reconfigured since having the active antennas change over time will require them to be frequently switched on and off, which would cause problems, especially in situations with high data rate. A revised algorithm is later presented that utilizes the mixed $l_{1,q}$ norm so that the locations of selected antennas in the array are kept the same between different sets of transmit symbols, with a weighting function modified accordingly. The chapter is finished with a detailed description of the revised algorithm, before presenting the simulation results acquired from a re-creation of the initial algorithm.

Main contribution of this thesis work is a novel algorithm for acquiring globally optimal solution for the beamforming problem of attaining maximum detection performance with a JRC system. A system model that is similar to the one in the previous chapter is used in this part of the work, although with major differences being the objective function based on SCNR rather than reference beam pattern and no direct path assumption being made between communication users which requires the channel to be modelled and included in the SNR expression for the communication operation. Assumptions about the system setting are similar to the work done in [7], albeit with a simplified clutter model that assumes only a single non-negligible clutter source. An objective function is built by dividing the signal power of the radar target return by the powers of noise and clutter return. Problem constraints consist of a power budget constraint that ensures the l_2 norm of transmitter beamforming weights is smaller than the available power, a receiver gain constraint that prevents the total array output power from changing by constraining the l_2 norm of receiver weight vector to be equal to 1, and a communication performance constraint that sets the SNR of communication operation to be equal to or larger than a given threshold value. This problem statement initially has two variables: the transmit beamforming weight vector and the receive beamforming weight vector. However, receive beamforming weights could be substituted by MVDR weights, leaving only the transmit beamforming weight vector as the optimization variable. Doing this substitution, and rephrasing the problem statement accordingly, results in the inverse matrix expression in the problem. The Sherman-Morrison formula is then used to convert the inverse matrix into a linear expression. The objective function is rephrased again after this by forming a matrix from the statements acquired from one of the constraints and then employing Schur's complement and its properties to convert the SCNR maximization constraint into a positive one semi-definiteness constraint which is a convex constraint function. Quadratic expressions of transmit beamforming vectors are rewritten as matrices to preserve convexity in the problem statement. If required, this process is reversed after acquiring a solution by utilizing rank reduction methods. The chapter concludes by presenting simulation results that depict the tradeoff between radar operation SCNR and communication operation SNR, along with how the approximation of orthogonality between array steering vectors pointing at different directions is affected by increasing the number of antenna elements in the array.

REFERENCES

[1] Chiriyath, A. R., Paul, B. and Bliss, D. W. Radar-Communications Convergence: Coexistence, Cooperation, and Co-Design. *IEEE Transactions on Cognitive Communications and Networking* 3.1 (2017), pp. 1–12. DOI: 10.1109/TCCN.2017.2666266.

[2] Damith Liyanaarachchi, S., Baquero Barneto, C., Riihonen, T., Heino, M. and Valkama, M. Joint Multi-User Communication and MIMO Radar Through Full-Duplex Hybrid Beamforming. *2021 1st IEEE International Online Symposium on Joint Communications & Sensing (JC&S)*. 2021, pp. 1–5. DOI: 10.1109/JCS52304.2021.9376319.

[3] Zhang, J. A., Liu, F., Masouros, C., Heath, R. W., Feng, Z., Zheng, L. and Petropulu, A. An Overview of Signal Processing Techniques for Joint Communication and Radar Sensing. *IEEE Journal of Selected Topics in Signal Processing* 15.6 (2021), pp. 1295–1315. DOI: 10.1109/JSTSP.2021.3113120.

[4] Zheng, L., Lops, M., Eldar, Y. C. and Wang, X. Radar and Communication Coexistence: An Overview: A Review of Recent Methods. *IEEE Signal Processing Magazine* 36.5 (2019), pp. 85–99. DOI: 10.1109/MSP.2019.2907329.

[5] Guo, H., Coetzee, S., Mason, D., Woodbridge, K. and Baker, C. Passive radar detection using wireless networks. *2007 IET International Conference on Radar Systems*. 2007, pp. 1–4. DOI: 10.1049/cp:20070643.

[6] Ahmed, A., Zhang, S. and Zhang, Y. D. Antenna Selection Strategy for transmit beamforming-based joint radar-communication system. *Digital Signal Processing* 105 (2020), p. 102768. DOI: 10.1016/j.dsp.2020.102768.

[7] Chen, L., Liu, F., Liu, J. and Masouros, C. *Composite Signalling for DFRC: Dedicated Probing Signal or Not?* 2020. DOI: 10.48550/ARXIV.2009.03528. URL: https://arxiv.org/abs/2009.03528.

[8] Mealey, R. M. A Method for Calculating Error Probabilities in a Radar Communication System. *IEEE Transactions on Space Electronics and Telemetry* 9.2 (1963), pp. 37–42. DOI: 10.1109/TSET.1963.4337601.

[9] Khozeimeh, F. and Haykin, S. Dynamic spectrum management for cognitive radio: an overview. *Wireless Communications and Mobile Computing* 9.11 (2009), pp. 1447–1459. DOI: https://doi.org/10.1002/wcm.732. eprint: https://onlinelibrary.wiley.com/doi/pdf/10.1002/wcm.732. URL: https://onlinelibrary.wiley.com/doi/abs/10.1002/wcm.732.

[10] Saruthirathanaworakun, R., Peha, J. M. and Correia, L. M. Opportunistic Sharing Between Rotating Radar and Cellular. *IEEE Journal on Selected Areas in Communications* 30.10 (2012), pp. 1900–1910. DOI: 10.1109/JSAC.2012.121106.

[11] Cianca, E., De Sanctis, M. and Di Domenico, S. Radios as Sensors. *IEEE Internet of Things Journal* 4.2 (2017), pp. 363–373. DOI: 10.1109/JIOT.2016.2563399.

[12] Kumari, P., Choi, J., González-Prelcic, N. and Heath, R. W. IEEE 802.11ad-Based Radar: An Approach to Joint Vehicular Communication-Radar System. *IEEE Transactions on Vehicular Technology* 67.4 (2018), pp. 3012–3027. DOI: 10.1109/TVT.2017.2774762.

[13] Daniels, R. C., Yeh, E. R. and Heath, R. W. Forward Collision Vehicular Radar With IEEE 802.11: Feasibility Demonstration Through Measurements. *IEEE Transactions on Vehicular Technology* 67.2 (2018), pp. 1404–1416. DOI: 10.1109/TVT.2017.2758581.

[14] Rahman, M. L., Zhang, J. A., Huang, X., Guo, Y. J. and Heath, R. W. Framework for a Perceptive Mobile Network Using Joint Communication and Radar Sensing. *IEEE Transactions on Aerospace and Electronic Systems* 56.3 (2020), pp. 1926–1941. DOI: 10.1109/TAES.2019.2939611.

[15] Liu, F., Masouros, C., Li, A. and Ratnarajah, T. Robust MIMO Beamforming for Cellular and Radar Coexistence. *IEEE Wireless Communications Letters* 6.3 (2017), pp. 374–377. DOI: 10.1109/LWC.2017.2693985.

[16] Martone, A. F., Gallagher, K. A. and Sherbondy, K. D. Joint Radar and Communication System Optimization for Spectrum Sharing. *2019 IEEE Radar Conference (RadarConf)*. 2019, pp. 1–6. DOI: 10.1109/RADAR.2019.8835700.

[17] Berger, C. R., Demissie, B., Heckenbach, J., Willett, P. and Zhou, S. Signal Processing for Passive Radar Using OFDM Waveforms. *IEEE Journal of Selected Topics in Signal Processing* 4.1 (2010), pp. 226–238. DOI: 10.1109/JSTSP.2009.2038977.

[18] Chetty, K., Smith, G. E. and Woodbridge, K. Through-the-Wall Sensing of Personnel Using Passive Bistatic WiFi Radar at Standoff Distances. *IEEE Transactions on Geoscience and Remote Sensing* 50.4 (2012), pp. 1218–1226. DOI: 10.1109/TGRS.2011.2164411.

[19] David, N., Sendik, Q., Messer, H. and Alpert, P. CELLULAR NETWORK INFRASTRUCTURE: The Future of Fog Monitoring? eng. *Bulletin of the American Meteorological Society* 96.10 (2015), pp. 1687–1698. ISSN: 0003-0007.

[20] Uijlenhoet, R., Overeem, A. and Leijnse, H. Opportunistic remote sensing of rainfall using microwave links from cellular communication networks. eng. *Wiley interdisciplinary reviews. Water* 5.4 (2018), e1289–e1289. ISSN: 2049-1948.

[21] Rossler, C. W., Ertin, E. and Moses, R. L. A software defined radar system for joint communication and sensing. *2011 IEEE RadarCon (RADAR)*. 2011, pp. 1050–1055. DOI: 10.1109/RADAR.2011.5960696.

[22] Ali, A., Gonzalez-Prelcic, N., Heath, R. W. and Ghosh, A. Leveraging Sensing at the Infrastructure for mmWave Communication. *IEEE Communications Magazine* 58.7 (2020), pp. 84–89. DOI: 10.1109/MCOM.001.1900700.

[23] Zhang, A., Rahman, M. L., Huang, X., Guo, Y. J., Chen, S. and Heath, R. W. Perceptive Mobile Networks: Cellular Networks With Radio Vision via Joint Communication and Radar Sensing. *IEEE Vehicular Technology Magazine* 16.2 (2021), pp. 20–30. DOI: 10.1109/MVT.2020.3037430.

[24] Paul, B., Chiriyath, A. R. and Bliss, D. W. Survey of RF Communications and Sensing Convergence Research. *IEEE Access* 5 (2017), pp. 252–270. DOI: 10.1109/ACCESS.2016.2639038.

[25] Bidigare, P. The Shannon channel capacity of a radar system. *Conference Record of the Thirty-Sixth Asilomar Conference on Signals, Systems and Computers, 2002.* Vol. 1. 2002, 113–117 vol.1. DOI: 10.1109/ACSSC.2002.1197159.

[26] Scheer, J., Melvin, W. L. and Aalfs, D. Chapter 9: Adaptive Digital Beamforming. *Principles of modern radar, Volume 2 - Advanced Techniques*. Institution of Engineering and Technology - IET, 2013, pp. 399–452.

[27] Van Veen, B. and Buckley, K. Beamforming: A versatile approach to spatial filtering. *IEEE ASSP Magazine* 5.2 (1988), pp. 4–24. DOI: 10.1109/53.665.

[28] Applebaum, S. and Chapman, D. Adaptive arrays with main beam constraints. *IEEE Transactions on Antennas and Propagation* 24.5 (1976), pp. 650–662. DOI: 10.1109/TAP.1976.1141416.

[29] Widrow, B., Mantey, P., Griffiths, L. and Goode, B. Adaptive antenna systems. *Proceedings of the IEEE* 55.12 (1967), pp. 2143–2159. DOI: 10.1109/PROC.1967.6092.

[30] Monzingo, R. A., Haupt, R. L. and Miller, T. W. Optimum Array Processing: Steady-State Performance Limits and the Wiener Solution. *Introduction to adaptive arrays*. SciTech Pub, 2011, pp. 92–98.

[31] Liu, F., Liu, Y.-F., Li, A., Masouros, C. and Eldar, Y. C. Cramér-Rao Bound Optimization for Joint Radar-Communication Beamforming. *IEEE Transactions on Signal Processing* 70 (2022), pp. 240–253. DOI: 10.1109/TSP.2021.3135692.

[32] Zhang, J. A., Huang, X., Guo, Y. J., Yuan, J. and Heath, R. W. Multibeam for Joint Communication and Radar Sensing Using Steerable Analog Antenna Arrays. *IEEE Transactions on Vehicular Technology* 68.1 (2019), pp. 671–685. DOI: 10.1109/TVT.2018.2883796.

[33] Luo, Y., Zhang, J. A., Huang, X., Ni, W. and Pan, J. Optimization and Quantization of Multibeam Beamforming Vector for Joint Communication and Radio Sensing. *IEEE Transactions on Communications* 67.9 (2019), pp. 6468–6482. DOI: 10.1109/TCOMM.2019.2923627.

[34] Luo, Y., Zhang, J. A., Huang, X., Ni, W. and Pan, J. Multibeam Optimization for Joint Communication and Radio Sensing Using Analog Antenna Arrays. *IEEE Transac-*

tions on Vehicular Technology 69.10 (2020), pp. 11000–11013. DOI: 10.1109/TVT.2020.3006481.

[35] Yuan, W., Liu, F., Masouros, C., Yuan, J., Ng, D. W. K. and González-Prelcic, N. Bayesian Predictive Beamforming for Vehicular Networks: A Low-Overhead Joint Radar-Communication Approach. *IEEE Transactions on Wireless Communications* 20.3 (2021), pp. 1442–1456. DOI: 10.1109/TWC.2020.3033776.

[36] Liu, F., Yuan, W., Masouros, C. and Yuan, J. Radar-Assisted Predictive Beamforming for Vehicular Links: Communication Served by Sensing. *IEEE Transactions on Wireless Communications* 19.11 (2020), pp. 7704–7719. DOI: 10.1109/TWC.2020.3015735.

[37] Boyd, S. P. and Vandenberghe, L. Convex functions. *Convex optimization*. Cambridge Univ. Pr., 2011, p. 67.

[38] Boyd, S. P. and Vandenberghe, L. Convex optimization problems. *Convex optimization*. Cambridge Univ. Pr., 2011, pp. 633–634.

[39] Grant, M. and Boyd, S. *CVX: Matlab Software for Disciplined Convex Programming, version 2.1*. http://cvxr.com/cvx. Mar. 2014.

[40] Grant, M. and Boyd, S. Graph implementations for nonsmooth convex programs. *Recent Advances in Learning and Control*. Ed. by V. Blondel, S. Boyd and H. Kimura. Lecture Notes in Control and Information Sciences. http://stanford.edu/~boyd/graph_dcp.html. Springer-Verlag Limited, 2008, pp. 95–110.

[41] Scheer, J. and Melvin, W. L. Chapter 10: Clutter Suppression Using Space-Time Adaptive Processing. *Principles of modern radar, Volume 2 - Advanced Techniques*. Institution of Engineering and Technology - IET, 2013, pp. 399–452.

[42] Melvin, W. L. and Scheer, J. A. Chapter 3: Radar Search and Overview of Detection in Interference. *Principles of modern radar, Volume 1 - Basic Principles*. SciTech Publishing, 2014, pp. 87–113.

[43] Sagnol, G. and Stahlberg, M. PICOS: A Python interface to conic optimization solvers. *Journal of Open Source Software* 7.70 (Feb. 2022), p. 3915. ISSN: 2475-9066. DOI: 10.21105/joss.03915.

[44] Van Veen, B. and Buckley, K. Beamforming: A versatile approach to spatial filtering. *IEEE ASSP Magazine* 5.2 (1988), pp. 4–24. DOI: 10.1109/53.665.

[45] Press, W. H., Teukolsky, S. A., Vetterling, W. T. and Flannery, B. P. Solution of Linear Algebraic Equations. *Numerical recipes: The art of scientific computing*. Cambridge University Press, 2007, pp. 76–79.

[46] Horn, R. A. and Zhang, F. Basic Properties of the Schur Complement. *The Schur Complement and Its Applications*. Ed. by F. Zhang. Boston, MA: Springer US, 2005, pp. 34–37. DOI: 10.1007/0-387-24273-2_2.

[47] Ayach, O. E., Heath, R. W., Abu-Surra, S., Rajagopal, S. and Pi, Z. The capacity optimality of beam steering in large millimeter wave MIMO systems. *2012 IEEE*

13th International Workshop on Signal Processing Advances in Wireless Communications (SPAWC). 2012, pp. 100–104. DOI: 10.1109/SPAWC.2012.6292865.

[48] Ai, W., Huang, Y. and Zhang, S. New results on Hermitian matrix rank-one decomposition. *Mathematical Programming* 128.1-2 (2009), pp. 253–283. DOI: 10.1007/s10107-009-0304-7.

[49] Huang, Y. and Zhang, S. Complex matrix decomposition and quadratic programming. *Mathematics of Operations Research* 32.3 (2007), pp. 758–768. DOI: 10.1287/moor.1070.0268.

[50] Sturm, J. F. and Zhang, S. On cones of nonnegative quadratic functions. *Mathematics of Operations Research* 28.2 (2003), pp. 246–267. DOI: 10.1287/moor.28.2.246.14485.

APPENDIX A: RANK REDUCTION METHODS

This appendix elaborates on algorithms for acquiring rank-one decomposition of Hermitian matrices. These methods are relevant for Chapter 4.4 in this thesis, where a rank-one matrix solution for the system of linear matrix equations defined by (4.68)-(4.71) is being sought. Dot operator is used for denoting inner product between matrices $\boldsymbol{A}$ and $\boldsymbol{B}$, such as $\boldsymbol{A} \bullet \boldsymbol{B} = Re\{tr(\boldsymbol{A}^H \boldsymbol{B})\}$ in this appendix.

A.1 Single matrix case

Let $\boldsymbol{A}$ be a Hermitian matrix of size n, and $\boldsymbol{X}$ be a positive semidefinite Hermitian matrix of size n and rank r. This decomposition relies on producing $\boldsymbol{x}$ vectors such that:

$$\boldsymbol{X} = \sum_{i=1}^{r} \boldsymbol{x}_i \boldsymbol{x}_i^H \tag{A.1}$$

$$\boldsymbol{x}_i^H \boldsymbol{A} \boldsymbol{x}_i = \frac{\boldsymbol{A} \bullet \boldsymbol{X}}{r} \tag{A.2}$$

Eigenvectors of $\boldsymbol{A}$ are used in generating $\boldsymbol{x}$ vectors.

- **Step 1:** Eigenvalues λ_i and eigenvectors $\boldsymbol{l}_i$ of X are acquired by eigenvalue decomposition. X can be built from those by $\boldsymbol{X} = \sum_{i=1}^{n} \lambda_i \boldsymbol{l}_i \boldsymbol{l}_i^H$.
- **Step 2:** If any those eigenvectors also satisfy $\lambda_i \boldsymbol{l}_i \boldsymbol{X} \boldsymbol{l}_i^H = \frac{\boldsymbol{A} \bullet \boldsymbol{X}}{r}$, it is one of the $\boldsymbol{x}$ vectors that satisfy (1) and (2). The process should be continued from step 5 in that case.
- **Step 3:** A pair of $\boldsymbol{u}_i = \sqrt{\lambda_i} \boldsymbol{l}_i$ are chosen such that $\boldsymbol{u}_1^H \boldsymbol{A} \boldsymbol{u}_1 > \frac{\boldsymbol{A} \bullet \boldsymbol{X}}{r}$, $\boldsymbol{u}_2^H \boldsymbol{A} \boldsymbol{u}_2 < \frac{\boldsymbol{A} \bullet \boldsymbol{X}}{r}$ and they are used for generating $\boldsymbol{v}_i = (\boldsymbol{u}_1 + \gamma \boldsymbol{u}_2)$. γ is found by solving the equation:

$$(\boldsymbol{u}_1 + \gamma \boldsymbol{u}_2)^H \boldsymbol{A} (\boldsymbol{u}_1 + \gamma \boldsymbol{u}_2) = (1 + \gamma^2) \frac{\boldsymbol{A} \bullet \boldsymbol{X}}{r} \tag{A.3}$$

which can be written in quadratic equation form:

$$\gamma^2(\boldsymbol{u}_2^H\boldsymbol{A}\boldsymbol{u}_2 - \frac{\boldsymbol{A}\bullet\boldsymbol{X}}{r}) + \gamma(\boldsymbol{u}_1^H\boldsymbol{A}\boldsymbol{u}_2 + \boldsymbol{u}_2^H\boldsymbol{A}\boldsymbol{u}_1) + \boldsymbol{u}_1^H\boldsymbol{A}\boldsymbol{u}_1 - \frac{\boldsymbol{A}\bullet\boldsymbol{X}}{r} = 0 \tag{A.4}$$

$$\gamma^2(\boldsymbol{u}_2^H\boldsymbol{A}\boldsymbol{u}_2 - \frac{\boldsymbol{A}\bullet\boldsymbol{X}}{r}) + 2\gamma Re\{\boldsymbol{u}_1^H\boldsymbol{A}\boldsymbol{u}_2\} + \boldsymbol{u}_1^H\boldsymbol{A}\boldsymbol{u}_1 - \frac{\boldsymbol{A}\bullet\boldsymbol{X}}{r} = 0 \tag{A.5}$$

It is known that the roots of this equation are real and have opposite signs from quadratic equation properties. Roots are acquired by the formula:

$$\gamma_1 = \frac{-2Re\{\boldsymbol{u}_1^H\boldsymbol{A}\boldsymbol{u}_2\} - \sqrt{\Delta}}{\boldsymbol{u}_1^H\boldsymbol{A}\boldsymbol{u}_2 - \frac{\boldsymbol{A}\bullet\boldsymbol{X}}{r}} \tag{A.6}$$

$$\gamma_2 = \frac{-2Re\{\boldsymbol{u}_1^H\boldsymbol{A}\boldsymbol{u}_2\} + \sqrt{\Delta}}{\boldsymbol{u}_1^H\boldsymbol{A}\boldsymbol{u}_2 - \frac{\boldsymbol{A}\bullet\boldsymbol{X}}{r}} \tag{A.7}$$

where, (A.8)

$$\Delta = 4\gamma Re\{\boldsymbol{u}_1^H\boldsymbol{A}\boldsymbol{u}_2\}^2 - 4(\boldsymbol{u}_1^H\boldsymbol{A}\boldsymbol{u}_1 - \frac{\boldsymbol{A}\bullet\boldsymbol{X}}{r})(\boldsymbol{u}_2^H\boldsymbol{A}\boldsymbol{u}_2 - \frac{\boldsymbol{A}\bullet\boldsymbol{X}}{r}) \tag{A.9}$$

- **Step 4:** The positive root is chosen among γ_1 and γ_2. Then another vector $\boldsymbol{v}$ is built by:

$$\boldsymbol{v} = \frac{\boldsymbol{u}_1 + \gamma\boldsymbol{u}_2}{\sqrt{1+\gamma^2}} \tag{A.10}$$

- **Step 5:** Acquired vector $\boldsymbol{v}$ is stored as the i^{th} $\boldsymbol{x}$ vector $\boldsymbol{x}_i$ and $\boldsymbol{X}$ matrix is updated as $\boldsymbol{X}' = \boldsymbol{X} - \boldsymbol{x}_i\boldsymbol{x}_i^H$. Previous steps are repeated while updating $\boldsymbol{X}$ at each iteration until r number of $\boldsymbol{z}$ vectors are acquired and $rank(\boldsymbol{X}) = 1$.

A.2 Two matrix case

This case could be thought of as the single matrix case applied two times over. Premises are same as the previous case, except there is an additional matrix $\boldsymbol{B}$ that is also Hermitian and of size n just like $\boldsymbol{A}$. This decomposition results in vectors $\boldsymbol{x}_i$ such that:

$$X = \sum_{i=1}^{r} \boldsymbol{x}_i\boldsymbol{x}_i^H \tag{A.11}$$

$$\boldsymbol{x}_i\boldsymbol{A}\boldsymbol{x}_i^H = \frac{\boldsymbol{A}\bullet\boldsymbol{X}}{r} \tag{A.12}$$

$$\boldsymbol{x}_i\boldsymbol{B}\boldsymbol{x}_i^H = \frac{\boldsymbol{B}\bullet\boldsymbol{X}}{r} \tag{A.13}$$

- **Step 1:** Single matrix decomposition is performed with $\boldsymbol{A}$ in order to acquire a set of vectors $\boldsymbol{u}_i$ such that:

$$\boldsymbol{X} = \sum_{i=1}^{r} \boldsymbol{u}_i \boldsymbol{u}_i^H \quad \text{(A.14)}$$

$$\boldsymbol{u}_i \boldsymbol{A} \boldsymbol{u}_i^H = \frac{\boldsymbol{A} \bullet \boldsymbol{X}}{r} \quad \text{(A.15)}$$

- **Step 2:** If any of those $\boldsymbol{u}_i$ vectors also satisfy $\boldsymbol{u}_i \boldsymbol{B} \boldsymbol{u}_i^H = \frac{\boldsymbol{B} \bullet \boldsymbol{X}}{r}$, then the process should be continued from step 5 where the vector to be stored will be $\boldsymbol{u}_i$.
- **Step 3:** Two vectors $\boldsymbol{u}_1^H \boldsymbol{B} \boldsymbol{u}_1 > \frac{\boldsymbol{B} \bullet \boldsymbol{X}}{r}$, $\boldsymbol{u}_2^H \boldsymbol{B} \boldsymbol{u}_2 < \frac{\boldsymbol{B} \bullet \boldsymbol{X}}{r}$ are found among $\boldsymbol{u}_i$, and they are used for generating $\boldsymbol{v}_i = (\boldsymbol{u}_1 + w\boldsymbol{u}_2)$. $w = \gamma e^{j\alpha}$ is a complex number which has its phase defined as $\alpha = \alpha_1 + \pi/2$ and its magnitude γ is found by solving the equation:

$$(\boldsymbol{u}_1 + w\boldsymbol{u}_2)^H \boldsymbol{A} (\boldsymbol{u}_1 + w\boldsymbol{u}_2) = (1 + \gamma^2) \frac{\boldsymbol{B} \bullet \boldsymbol{X}}{r} \quad \text{(A.16)}$$

which can be written in quadratic equation form:

$$|w|^2 (\boldsymbol{u}_2^H \boldsymbol{B} \boldsymbol{u}_2 - \frac{\boldsymbol{B} \bullet \boldsymbol{X}}{r}) + w \boldsymbol{u}_1^H \boldsymbol{B} \boldsymbol{u}_2 + \overline{w} \boldsymbol{u}_2^H \boldsymbol{A} \boldsymbol{u}_1 + \boldsymbol{u}_1^H \boldsymbol{A} \boldsymbol{u}_1 - \frac{\boldsymbol{B} \bullet \boldsymbol{X}}{r} = 0 \quad \text{(A.17)}$$

The expression $\boldsymbol{u}_2^H \boldsymbol{B} \boldsymbol{u}_1$ is a complex scalar and is represented as $\gamma_p e^{j\alpha_2}$ after this point.

$$\gamma^2 (\boldsymbol{u}_2^H \boldsymbol{B} \boldsymbol{u}_2 - \frac{\boldsymbol{B} \bullet \boldsymbol{X}}{r}) + \gamma e^{j\alpha} \gamma_p e^{-j\alpha_2} + \gamma e^{-j\alpha} \gamma_p e^{j\alpha_2} + \boldsymbol{u}_1^H \boldsymbol{A} \boldsymbol{u}_1 - \frac{\boldsymbol{A} \bullet \boldsymbol{X}}{r} = 0 \quad \text{(A.18)}$$

$$\gamma^2 (\boldsymbol{u}_2^H \boldsymbol{B} \boldsymbol{u}_2 - \frac{\boldsymbol{B} \bullet \boldsymbol{X}}{r}) + \gamma_p \gamma (e^{j\alpha} e^{-j\alpha_2} + e^{-j\alpha} e^{j\alpha_2}) + \boldsymbol{u}_1^H \boldsymbol{A} \boldsymbol{u}_1 - \frac{\boldsymbol{A} \bullet \boldsymbol{X}}{r} = 0 \quad \text{(A.19)}$$

$$\gamma^2 (\boldsymbol{u}_2^H \boldsymbol{B} \boldsymbol{u}_2 - \frac{\boldsymbol{B} \bullet \boldsymbol{X}}{r}) + 2\gamma_p \gamma cos(\alpha - \alpha_2) + \boldsymbol{u}_1^H \boldsymbol{A} \boldsymbol{u}_1 - \frac{\boldsymbol{A} \bullet \boldsymbol{X}}{r} = 0 \quad \text{(A.20)}$$

$$\gamma^2 (\boldsymbol{u}_2^H \boldsymbol{B} \boldsymbol{u}_2 - \frac{\boldsymbol{B} \bullet \boldsymbol{X}}{r}) + 2\gamma_p \gamma cos(\alpha_1 + \pi/2 - \alpha_2) + \boldsymbol{u}_1^H \boldsymbol{A} \boldsymbol{u}_1 - \frac{\boldsymbol{A} \bullet \boldsymbol{X}}{r} = 0 \quad \text{(A.21)}$$

$$\gamma^2 (\boldsymbol{u}_2^H \boldsymbol{B} \boldsymbol{u}_2 - \frac{\boldsymbol{B} \bullet \boldsymbol{X}}{r}) + 2\gamma_p \gamma sin(\alpha_2 - \alpha_1) + \boldsymbol{u}_1^H \boldsymbol{A} \boldsymbol{u}_1 - \frac{\boldsymbol{A} \bullet \boldsymbol{X}}{r} = 0 \quad \text{(A.22)}$$

It is known that the roots of this equation are real and have opposite signs from quadratic equation properties. Roots are acquired by the formula:

$$\gamma_1 = \frac{-2\gamma_p sin(\alpha_2 - \alpha_1) - \sqrt{\Delta}}{2(\boldsymbol{u}_2^H \boldsymbol{B}\boldsymbol{u}_2 - \frac{\boldsymbol{B}\bullet\boldsymbol{X}}{r})} \tag{A.23}$$

$$\gamma_2 = \frac{-2\gamma_p sin(\alpha_2 - \alpha_1) + \sqrt{\Delta}}{2(\boldsymbol{u}_2^H \boldsymbol{B}\boldsymbol{u}_2 - \frac{\boldsymbol{B}\bullet\boldsymbol{X}}{r})} \tag{A.24}$$

$$\Delta = 4(\gamma_p sin(\alpha_2 - \alpha_1))^2 - 4(\boldsymbol{u}_1^H \boldsymbol{B}\boldsymbol{u}_1 - \frac{\boldsymbol{B}\bullet\boldsymbol{X}}{r})(\boldsymbol{u}_2^H \boldsymbol{B}\boldsymbol{u}_2 - \frac{\boldsymbol{B}\bullet\boldsymbol{X}}{r}) \tag{A.25}$$

- **Step 4:** The positive root is chosen among γ_1 and γ_2 to be named γ. Then two other vectors $\boldsymbol{v}_1$ and $\boldsymbol{v}_2$ are built by:

$$\boldsymbol{v}_1 = \frac{\boldsymbol{u}_1 + w\boldsymbol{u}_2}{\sqrt{1+\gamma^2}} \tag{A.26}$$

$$\boldsymbol{v}_2 = \frac{\overline{w}\boldsymbol{u}_1 - \boldsymbol{u}_2}{\sqrt{1+\gamma^2}} \tag{A.27}$$

- **Step 5:** The vector $\boldsymbol{v}_1$ is stored as the i^{th} $\boldsymbol{x}$ vector $\boldsymbol{x}_i$, and update $\boldsymbol{X}$ matrix as $\boldsymbol{X}' = \boldsymbol{X} - \boldsymbol{x}_i\boldsymbol{x}_i^H$. Previous steps are repeated while updating $\boldsymbol{X}$ at each iteration until r number of $\boldsymbol{x}$ vectors are acquired and $rank(\boldsymbol{X}) = 1$.

A.3 Three matrix case

In this case, there are three Hermitian matrices $\boldsymbol{A}$, $\boldsymbol{B}$, and $\boldsymbol{C}$, of size n, in addition to a nonzero Hermitian positive semidefinite matrix $\boldsymbol{X}$ of size n and rank r. Assuming that $r \geq 3$ it is possible to find a rank one decomposition of $\boldsymbol{X}$, $\boldsymbol{X} = \sum_{i=1}^{r} \boldsymbol{y}_i\boldsymbol{y}_i^H$, such that:

$$\boldsymbol{A}\bullet\boldsymbol{y}_i\boldsymbol{y}_i^H = \boldsymbol{A}\bullet X/r, \qquad i = 1,\ldots,r; \tag{A.28}$$

$$\boldsymbol{B}\bullet\boldsymbol{y}_i\boldsymbol{y}_i^H = \boldsymbol{B}\bullet X/r, \qquad i = 1,\ldots,r; \tag{A.29}$$

$$\boldsymbol{C}\bullet\boldsymbol{y}_i\boldsymbol{y}_i^H = \boldsymbol{C}\bullet X/r, \qquad i = 1,\ldots,r-2; \tag{A.30}$$

Likewise, in the previous case, the decomposition for $\boldsymbol{A}$ and $\boldsymbol{B}$ is performed by employing the methods for one and two matrix cases. Then, acquired vectors are utilized to form an equation, resulting in another vector that will satisfy it for $\boldsymbol{C}$. However, there are three equations to satisfy this time, requiring an equation system with three unknowns to acquire a solution.

- **Step 1:** Decomposition for two matrices is applied on $\boldsymbol{A}$ and $\boldsymbol{B}$ to acquire a set of

$\boldsymbol{x}$ vectors such that:

$$\boldsymbol{X} = \sum_{i=1}^{r} \boldsymbol{x}_i \boldsymbol{x}_i^H \tag{A.31}$$

$$\boldsymbol{A} \bullet \boldsymbol{x}_i \boldsymbol{x}_i^H = \boldsymbol{A} \bullet \boldsymbol{X}/r \tag{A.32}$$

$$\boldsymbol{B} \bullet \boldsymbol{x}_i \boldsymbol{x}_i^H = \boldsymbol{B} \bullet \boldsymbol{X}/r \tag{A.33}$$

for all $i = 1, \ldots, r$. The notation $\delta_a = \boldsymbol{A} \bullet \boldsymbol{X}$, $\delta_b = \boldsymbol{B} \bullet \boldsymbol{X}$, and $\delta_c = \boldsymbol{C} \bullet \boldsymbol{X}$ will be used from now on for simplicity.

- **Step 2:** If any of those $\boldsymbol{x}_i$ vectors also satisfy $\boldsymbol{C} \bullet \boldsymbol{x}_i \boldsymbol{x}_i^H = \delta_c/r$, process should be continued from step 5 by storing that $\boldsymbol{x}_i$ as one of the $\boldsymbol{y}$ vectors.
- **Step 3:** One of the $\boldsymbol{x}$ vectors is chosen so that $\boldsymbol{C} \bullet \boldsymbol{x}_1 \boldsymbol{x}_1^H - \delta_c/r > 0$, another one is chosen so that $\boldsymbol{C} \bullet \boldsymbol{x}_2 \boldsymbol{x}_2^H - \delta_c/r < 0$, and a different third vector $\boldsymbol{x}_3$ is freely chosen. Vector $\boldsymbol{y}$ is calculated as a normalized linear combination of those three vectors:

$$\boldsymbol{y} = \frac{\alpha_1 \boldsymbol{x}_1 + \alpha_2 \boldsymbol{x}_2 + \alpha_3 \boldsymbol{x}_3}{\sqrt{|\alpha_1|^2 + |\alpha_2|^2 + |\alpha_3|^2}} \tag{A.34}$$

where α_1, α_2, and α_3 are the three unknowns to be calculated. The equation system is formed as follows:

$$\boldsymbol{A} \bullet \boldsymbol{y}\boldsymbol{y}^H = \delta_a/r \tag{A.35}$$

$$\boldsymbol{B} \bullet \boldsymbol{y}\boldsymbol{y}^H = \delta_b/r \tag{A.36}$$

$$\boldsymbol{C} \bullet \boldsymbol{y}\boldsymbol{y}^H = \delta_c/r \tag{A.37}$$

These expressions will be rewritten for clarity purposes. (A.35) can be written in the form:

$$\boldsymbol{A} \bullet \boldsymbol{y}\boldsymbol{y}^H = Re\{tr(\boldsymbol{y}^H \boldsymbol{A} \boldsymbol{y})\} \tag{A.38}$$

$$= \delta_a/r \tag{A.39}$$

Substituting $\boldsymbol{y}$ with (A.34) yields:

$$\delta_a/r = Re\{tr((\frac{\alpha_1 \boldsymbol{x}_1 + \alpha_2 \boldsymbol{x}_2 + \alpha_3 \boldsymbol{x}_3}{\sqrt{|\alpha_1|^2 + |\alpha_2|^2 + |\alpha_3|^2}})^H \boldsymbol{A} \frac{\alpha_1 \boldsymbol{x}_1 + \alpha_2 \boldsymbol{x}_2 + \alpha_3 \boldsymbol{x}_3}{\sqrt{|\alpha_1|^2 + |\alpha_2|^2 + |\alpha_3|^2}})\} \tag{A.40}$$

$$= \frac{1}{|\alpha_1|^2 + |\alpha_2|^2 + |\alpha_3|^2} Re\{tr((\alpha_1 \boldsymbol{x}_1 + \alpha_2 \boldsymbol{x}_2 + \alpha_3 \boldsymbol{x}_3)^H \boldsymbol{A} (\alpha_1 \boldsymbol{x}_1 + \alpha_2 \boldsymbol{x}_2 + \alpha_3 \boldsymbol{x}_3))\} \tag{A.41}$$

Multiplying both sides with $|\alpha_1|^2 + |\alpha_2|^2 + |\alpha_3|^2$ and proceeding with operations leads to:

$$\begin{aligned}Re\{|\alpha_1|^2\boldsymbol{x}_1^H\boldsymbol{A}\boldsymbol{x}_1 + \overline{\alpha}_1\alpha_2\boldsymbol{x}_1^H\boldsymbol{A}\boldsymbol{x}_2 + \overline{\alpha}_1\alpha_3\boldsymbol{x}_1^H\boldsymbol{A}\boldsymbol{x}_3 + \dots\\ \overline{\alpha}_2\alpha_1\boldsymbol{x}_2^H\boldsymbol{A}\boldsymbol{x}_1 + |\alpha_2|^2\boldsymbol{x}_2^H\boldsymbol{A}\boldsymbol{x}_2 + \overline{\alpha}_2\alpha_3\boldsymbol{x}_2^H\boldsymbol{A}\boldsymbol{x}_3 + \dots\\ \overline{\alpha}_3\alpha_1\boldsymbol{x}_3^H\boldsymbol{A}\boldsymbol{x}_1 + \overline{\alpha}_3\alpha_2\boldsymbol{x}_3^H\boldsymbol{A}\boldsymbol{x}_2 + |\alpha_3|^2\boldsymbol{x}_3^H\boldsymbol{A}\boldsymbol{x}_3\}\\ = (|\alpha_1|^2 + |\alpha_2|^2 + |\alpha_3|^2)\delta_a/r\end{aligned}$$

It is theoretically known that $\boldsymbol{n}^H\boldsymbol{M}\boldsymbol{n}$ is real for any complex $\boldsymbol{n}$ vector. Therefore terms with $|\alpha_i|^2$ can be taken out of $Re\{\dots\}$ parenthesis. δ_a could be substituted with $\boldsymbol{A} \bullet \boldsymbol{x}_i\boldsymbol{x}_i^H = \boldsymbol{x}_i^H\boldsymbol{A}\boldsymbol{x}$ for any $i = 1, 2, 3$. Thus $|\alpha_i|^2$ terms could be eliminated by subtracting the right hand side from both sides:

$$\begin{aligned}Re\{\overline{\alpha}_1\alpha_2\boldsymbol{x}_1^H\boldsymbol{A}\boldsymbol{x}_2 + \overline{\alpha}_1\alpha_3\boldsymbol{x}_1^H\boldsymbol{A}\boldsymbol{x}_3 + \overline{\alpha}_2\alpha_1\boldsymbol{x}_2^H\boldsymbol{A}\boldsymbol{x}_1 + \dots\\ \overline{\alpha}_2\alpha_3\boldsymbol{x}_2^H\boldsymbol{A}\boldsymbol{x}_3 + \overline{\alpha}_3\alpha_1\boldsymbol{x}_3^H\boldsymbol{A}\boldsymbol{x}_1 + \overline{\alpha}_3\alpha_2\boldsymbol{x}_3^H\boldsymbol{A}\boldsymbol{x}_2\} = 0\end{aligned}$$

Now it should be observed that $(\overline{\alpha}_1\alpha_2\boldsymbol{x}_1^H\boldsymbol{A}\boldsymbol{x}_2)^H = \overline{\alpha}_2\alpha_1\boldsymbol{x}_2^H\boldsymbol{A}\boldsymbol{x}_1$, $(\overline{\alpha}_1\alpha_3\boldsymbol{x}_1^H\boldsymbol{A}\boldsymbol{x}_3)^H = \overline{\alpha}_3\alpha_1\boldsymbol{x}_3^H\boldsymbol{A}\boldsymbol{x}_1$, and $(\overline{\alpha}_2\alpha_3\boldsymbol{x}_2^H\boldsymbol{A}\boldsymbol{x}_3)^H = \overline{\alpha}_3\alpha_2\boldsymbol{x}_3^H\boldsymbol{A}\boldsymbol{x}_2$. Noting that each of these terms are scalar and taking the Hermitian of a scalar is equivalent to taking their complex conjugate, the property $z + \overline{z} = 2Re\{z\}$ could be used to rewrite the equation as:

$$2Re\{\overline{\alpha}_1\alpha_2\boldsymbol{x}_1^H\boldsymbol{A}\boldsymbol{x}_2\} + 2Re\{\overline{\alpha}_1\alpha_3\boldsymbol{x}_1^H\boldsymbol{A}\boldsymbol{x}_3\} + 2Re\{\overline{\alpha}_2\alpha_3\boldsymbol{x}_2^H\boldsymbol{A}\boldsymbol{x}_3\} = 0. \quad \text{(A.42)}$$

Seeking the exact same steps with (A.36) results in:

$$2Re\{\overline{\alpha}_1\alpha_2\boldsymbol{x}_1^H\boldsymbol{B}\boldsymbol{x}_2\} + 2Re\{\overline{\alpha}_1\alpha_3\boldsymbol{x}_1^H b\boldsymbol{x}_3\} + 2Re\{\overline{\alpha}_2\alpha_3\boldsymbol{x}_2^H\boldsymbol{B}\boldsymbol{x}_3\} = 0 \quad \text{(A.43)}$$

(A.37) follows likewise, but $|\alpha_i|^2$ terms cannot be eliminated since $\delta_c \neq \boldsymbol{x}_i^H\boldsymbol{C}\boldsymbol{x}_i$. It becomes:

$$\begin{aligned}(\boldsymbol{x}_1^H\boldsymbol{C}\boldsymbol{x}_1 - \delta_c/r)|\alpha_1|^2 + (\boldsymbol{x}_2^H\boldsymbol{C}\boldsymbol{x}_2 - \delta_c/r)|\alpha_2|^2 + (\boldsymbol{x}_3^H\boldsymbol{C}\boldsymbol{x}_3 - \delta_c/r)|\alpha_3|^2 + \dots\\ 2Re\{\boldsymbol{x}_1^H\boldsymbol{C}\boldsymbol{x}_2\overline{\alpha}_1\alpha_2\} + 2Re\{\boldsymbol{x}_2^H\boldsymbol{C}\boldsymbol{x}_3\overline{\alpha}_2\alpha_3 + 2Re\{\boldsymbol{x}_3^H\boldsymbol{C}\boldsymbol{x}_1\overline{\alpha}_3\alpha_1\} = 0\end{aligned}$$

- **Step 4:** It is theoretically known that this system of equations has a nonzero solution. Acquiring the values of α_1, α_2, α_3, possibly by employing a solver tool and substituting them in (A.34) yields one of the $\boldsymbol{y}$ vectors.
- **Step 5:** Acquired vector is stored as i^{th} $\boldsymbol{y}$ vector $\boldsymbol{y}_i$, and $\boldsymbol{X}$ is updated as $\boldsymbol{X}' = \boldsymbol{X} - \boldsymbol{y}_i\boldsymbol{y}_i^H$. Previous steps are repeated until $rank(\boldsymbol{X}) = 2$, and two matrix decomposition is applied on $\boldsymbol{A}$ and $\boldsymbol{B}$ that point to complete the rank reduction process for those. $\boldsymbol{C}$ can only be decomposed until rank of $\boldsymbol{X}$ is reduced to 2 by

this method. However, a similar theorem also works for this situation, which gets utilized in the four matrix case.

A.4 Four matrix case

The rank-one decompositions for one and two matrix cases and a theorem similar to rank-one decomposition for three matrix cases are utilized for this case. The relevant theorem is mentioned in Step 2. This case is different from the previous three in the sense that instead of performing a complete rank-one decomposition of $\boldsymbol{X}$, a rank-one matrix solution for the following system of linear matrix equations is being sought:

$$\boldsymbol{A} \bullet \boldsymbol{z}\boldsymbol{z}^H = \boldsymbol{A} \bullet \boldsymbol{X} \tag{A.44}$$

$$\boldsymbol{B} \bullet \boldsymbol{z}\boldsymbol{z}^H = \boldsymbol{B} \bullet \boldsymbol{X} \tag{A.45}$$

$$\boldsymbol{C} \bullet \boldsymbol{z}\boldsymbol{z}^H = \boldsymbol{C} \bullet \boldsymbol{X} \tag{A.46}$$

$$\boldsymbol{D} \bullet \boldsymbol{z}\boldsymbol{z}^H = \boldsymbol{D} \bullet \boldsymbol{X} \tag{A.47}$$

where $\boldsymbol{A}$, $\boldsymbol{B}$, $\boldsymbol{C}$, and $\boldsymbol{D}$ are Hermitian matrices of size n with $n \geq 3$, and $\boldsymbol{X}$ is a nonzero Hermitian positive semidefinite matrix of rank r. A nonzero vector z that satisfies this equation system could be found provided that the vector containing the results of operations $\boldsymbol{A} \bullet \boldsymbol{X}$, $\boldsymbol{B} \bullet \boldsymbol{X}$, $\boldsymbol{C} \bullet \boldsymbol{X}$, $\boldsymbol{D} \bullet \boldsymbol{X}$ is not a zero vector. A rephrasing in the form of $\boldsymbol{A} \bullet \boldsymbol{X} = \delta_a$ will be used for all four matrices in the system of linear matrix equations in this subsection of the appendix.

- **Step 1:** Any nonzero δ is chosen among δ_a, δ_b, δ_c, and δ_d. We know that at least one of them should be nonzero. Let us choose δ_d for this example.
- **Step 2:** According to "Theorem 2.2" in [48], given three Hermitian matrices $\boldsymbol{M}_1$, $\boldsymbol{M}_2$, $\boldsymbol{M}_3$ of size n, and a nonzero Hermitian positive semmidefinite matrix $\boldsymbol{X}$ of size n and rank r, a nonzero vector $\boldsymbol{y}$ can be found such that:

$$\boldsymbol{M}_1 \bullet \boldsymbol{y}\boldsymbol{y}^H = \boldsymbol{M}_1 \bullet \boldsymbol{X} \tag{A.48}$$

$$\boldsymbol{M}_2 \bullet \boldsymbol{y}\boldsymbol{y}^H = \boldsymbol{M}_2 \bullet \boldsymbol{X} \tag{A.49}$$

$$\boldsymbol{M}_3 \bullet \boldsymbol{y}\boldsymbol{y}^H = \boldsymbol{M}_3 \bullet \boldsymbol{X} \tag{A.50}$$

as long as $r \geq 2$. Applying this theorem to matrices $\boldsymbol{M}_1 = \boldsymbol{A} - \frac{\delta_a}{\delta_d}\boldsymbol{D}$, $\boldsymbol{M}_2 = \boldsymbol{B} - \frac{\delta_b}{\delta_d}\boldsymbol{D}$, and $\boldsymbol{M}_3 = \boldsymbol{C} - \frac{\delta_c}{\delta_d}\boldsymbol{D}$ results in a nonzero n dimensional complex vector

$\boldsymbol{y}$ such that:

$$\boldsymbol{y}^H(\boldsymbol{A} - \frac{\delta_a}{\delta_d}\boldsymbol{D})\boldsymbol{y} = (\boldsymbol{A} - \frac{\delta_a}{\delta_d}\boldsymbol{D}) \bullet \boldsymbol{X} = 0 \tag{A.51}$$

$$\boldsymbol{y}^H(\boldsymbol{B} - \frac{\delta_b}{\delta_d}\boldsymbol{D})\boldsymbol{y} = (\boldsymbol{B} - \frac{\delta_b}{\delta_d}\boldsymbol{D}) \bullet \boldsymbol{X} = 0 \tag{A.52}$$

$$\boldsymbol{y}^H(\boldsymbol{C} - \frac{\delta_c}{\delta_d}\boldsymbol{D})\boldsymbol{y} = (\boldsymbol{C} - \frac{\delta_c}{\delta_d}\boldsymbol{D}) \bullet \boldsymbol{X} = 0. \tag{A.53}$$

- **Step 3:** Using the denotation $t = \frac{\boldsymbol{y}^H\boldsymbol{D}\boldsymbol{y}}{\delta_d}$ leads to:

$$\boldsymbol{y}^H\boldsymbol{A}\boldsymbol{y} = t\delta_a \tag{A.54}$$

$$\boldsymbol{y}^H\boldsymbol{B}\boldsymbol{y} = t\delta_b \tag{A.55}$$

$$\boldsymbol{y}^H\boldsymbol{C}\boldsymbol{y} = t\delta_c \tag{A.56}$$

$$\boldsymbol{y}^H\boldsymbol{D}\boldsymbol{y} = t\delta_d. \tag{A.57}$$

- **Step 4:** The vector $\mathbf{z}$ that was being sought is equal to $\frac{\boldsymbol{y}}{\sqrt{t}}$ as it could be seen from the previous step.